JOURNAL OF MECHANICS OF CONTINUA AND MATHEMATICAL SCIENCES
www.journalimcms.org

ISSN (Online) : 2454 -7190 Vol.-21, No.-11, November (2026) pp 131-165 ISSN (Print) 0973-8975

A HYBRID INVERSE GOMPERTZ–SVM FRAMEWORK FOR RELIABILITY-ORIENTED SURVIVAL MODELLING OF CANCER DATA

Ameena K. Essa[1], Asmaa A.Mahdi [2], Hasanain Jalil Neamah Alsaedi [3], Adel S. Hussain[4], Rana Aziz Yousif Almuttalibi[5]

[1]Mustansiriyah University, Baghdad, Iraq.Emai:

[2,3] University Information Technology and Communication, Baghdad, Iraq.

[3]Mustansiriyah University, Baghdad, Iraq.

[4]Department of IT, Amedi Technical Institutes, University of Duhok Polytechnic, Duhok, Iraq.

[4]Department of Administrative and Financial Affairs, Faculty Division, Al-Iraqi University, Baghdad, Iraq.

[4]Department of Computer Engineering, Al-Kitab University, Altun, Kupri, Kirkuk, Iraq.

[5]University Information Technology and Communication, Baghdad, Iraq.

Email: [1]ameena@uomstansiriyah.edu.iq, [2]asmaa.mahdi@uoitc.edu.iq, [3]Hasanien.1975@uoitc.edu.iq, [4]Adel.sufyan@dpu.edu.krd, [5]Rana.aziz@uoitc.edu.iq

Corresponding Author: **Hasanain Jalil Neamah Alsaedi**

https://doi.org/10.26782/jmcms.2026.11.00007

(Received: May 25, 2026; Revised: October 10, 2026; Accepted: November 02, 2026)

Abstract

This paper investigates the Inverse Gompertz (IG) distribution as a parametric model for cancer survival durations and analyzes support vector regression (SVR) as a numerical surrogate for several IG-based reliability functionals. The IG parameters are calculated by maximum likelihood. RBF-kernel SVR models are then shown as approximating the probability density, survival, and hazard functions created by the fitted distribution. A simulation component looks at sample sizes of 50, 100, 500, and 1,000. The application component is stated as including 50 breast-cancer and 100 brain-cancer observations. The provided results show that the IG distribution can be a flexible descriptive representation of observed event-time distributions. However, as the SVR targets are derived from the fitted IG model, SVR approximation error does not provide independent evidence for increased patient-level prognostic accuracy. The clinical analyzes are further constrained by the stated absence of right-censored observations, lack of patient-level variables, and insufficient reporting of cohort definitions and validation procedures. The findings should therefore be viewed as a methodological demonstration rather than a clinically proven predictive system.

Keywords: Survival analysis; Inverse Gompertz distribution; maximum likelihood estimation; support vector regression; reliability functionals; cancer data.

I. Introduction

Cancer survival analysis is the study of the period from a well-defined origin (diagnosis or start of treatment) to a specific event, which is most typically death or disease recurrence. Appropriate analysis requires a specific definition of the time origin, event, follow-up period, and censoring technique. Parametric lifespan distributions can give a succinct description of event-time distributions, but are effective only when their assumptions are in agreement with the data seen [I-X]. The Kaplan–Meier estimator and Cox proportional-hazards model are standard approaches for time-to-event analysis. Parametric alternatives can be useful when there is substantial knowledge and diagnostics that support a proper distributional form. They have the advantage of interpretable survival and hazard functions and the main danger of model misspecification. A parametric distribution should then be checked using graphical and numerical diagnostics and contrasted with plausible alternatives rather than picked simply because it can provide a flexible hazard curve. Since the parametrization of the Inverse Gompertz (IG) distribution allows for describing non-constant hazard patterns, we explore it as a possible model for longevity. The appropriateness of the distribution is an empirical concern. Theoretical flexibility does not show that a certain hazard shape exists in a certain cancer cohort. Hence, parameter estimation, goodness-of-fit assessment, and uncertainty quantification are crucial to the analysis.

The kernel functions allow support vector regression (SVR) to approximate nonlinear input-output relationships. In this publication, however, SVR is stated as learning the relationship between time and functionals created from an IG model adapted using maximum likelihood. This is a proxy modeling problem, not direct learning from patient-level predictors and outcomes. Thus, IG-generated targets cannot by themselves be shown to better predict survival for new patients [X-XX]. The aims are to characterize the IG distribution and its reliability functionals, estimate its parameters by maximum likelihood, explore the capability of an RBF-kernel SVR to approximate selected IG-derived functions, and demonstrate the workflow on the two presented cancer datasets. The study does not provide a validated clinical prediction tool.

The methodological contribution is the assessment of an SVR surrogate for selected functionals from an IG parametric model. The surrogate can be convenient computationally for repetitive function evaluation, but it should not be treated as an independent survival estimator unless trained and evaluated against patient-level outcomes in a leakage-free manner.

The investigation also compares the IG model with other lifespan distributions using probability-based criteria and graphical diagnostics where available. Such comparisons are only valid if all candidate distributions are fitted to the same observations, have comparable likelihood criteria and are evaluated on the same time scale. The simulation study considers estimating behavior for a number of sample sizes. The results of the simulations depend on the assumed data-generating distribution and parameter values and should not be applied to arbitrary clinical populations or regarded as evidence of superiority under model misspecification.

The real-data part is said to be composed of two retrospective datasets (50 breast-cancer patients and 100 brain-cancer cases). The description supplied suggests entire event times, but confirmation is needed for the event status, time origin, completeness of follow-up, and inclusion criteria before the analyzes can be considered as survival analyzes.

The primary claims are consequently limited to distributional fit and numerical approximation. Clinical interpretation is confined to description of fitted curves in the population; no causal treatment effects, individual risk scores or treatment suggestions are inferred.

The remainder of the work is organized as follows: the IG model and its reliability functions, the estimate and SVR techniques, the simulation design, the clinical data descriptions, the numerical results, and the limitations.

- An integrated hybrid modelling approach is established incorporating the Inverse Gompertz (IG) distribution using the Support Vector Machine (SVM) regression in estimating reliability-based survival functionals.
- A thorough comparative study of clinical Maximum Likelihood Estimation (MLE) and SVM-based predictive modelling compares their performance in estimating the survival-related measures.
- A simulation study is conducted on a large scale to determine the performance of estimators based on various sample sizes in terms of Root Mean Square Error (RMSE) and bias.

Just like other related research, the suggested IG-SVM framework is implemented on actual survival data of breast and brain cancer patients to show that it can be practically used to model biomedical survival dynamics.

The present paper adds to the various intersections between reliable theory, survival analysis, and machine learning with the introduction of a hybrid modelling framework consisting of the Inverse Gompertz (IG) distribution and Support Vector Machine (SVM) regression to predict the survival-related functionalities. Though some parametric lifetime models, including Weibull, log-logistic, and Burr families, were actively used in both survival modelling and reliability analysis to model different types of behaviours of hazard rates [I-XXX], the introduction of a machine learning approach to these parametric models is rather scarce. Specifically, whereas artificial neural networks, convolutional neural networks, and other machine learning algorithms have lately been applied to predict survival and model medical prognosis [citation to verify], the application of Support Vector Machines in the context of the Inverse Gompertz has not been studied systematically.

The primary research issue that the study is devoted to is the deficit of using machine learning methods and parametric lifetime distributions to estimate reliability-based survival functionals. Hence, the major idea of the present study is to design and test a hybrid modelling system integrating the Inverse Gompertz distribution with Support Vector Machine regression in the prediction of the survival behaviour of cancer patients.

More precisely, this work gives a systematic review of classical Maximum Likelihood Estimation (MLE) and SVM-based predictive modelling in approximating major

reliability-oriented survival measures, such as the survival function and the hazard rate. To further assess the suggested method, a comprehensive simulation experiment is conducted under varying sample sizes with the use of Root Mean Square Error (RMSE) and bias as the performance measures. Lastly, IG -SVM framework is put into practice using actual survival data of breast and brain cancer patients to showcase its potential usefulness in the modelling of intricate biomedical survival dynamics.

The novelty of this work does not lie in proposing a new probability distribution. Rather, it lies in examining an SVR surrogate for selected functionals derived from an IG parametric model and illustrating the workflow with two reported cancer datasets. Any claim of improved predictive performance must account for the fact that the SVR targets are generated by the IG model itself.

II. The Inverse Gompertz distribution (Proposed Model)

The CDF of the random variable Y under the Inverse Gompertz distribution, α and β are the shape and scale parameters, respectively, can be used to describe the probability that the survival time will not be greater than some given time t.

$$F(y|\alpha,\beta) = \exp\left[-\alpha\left(e^{\frac{\beta}{y}} - 1\right)\right];\ \ y > 0, \alpha, \beta > 0. \tag{1}$$

And the PDF of the Inverse Gompertz distribution is:

$$f(y|\alpha,\beta) = \frac{\alpha\beta}{y^2}\exp\left(\frac{\beta}{y}\right)\exp\left[-\alpha\left(e^{\frac{\beta}{y}} - 1\right)\right]; y > 0, \alpha, \beta > 0. \tag{2}$$

The Inverse Gompertz distribution can be used in various research areas because of its capability to overcome the distributional irregularities format, as shown in Figure 1(a-f). It is especially applicable both in theoretical development and practical analysis in time-to-event data settings because of its flexibility in modelling various patterns of hazard rates.

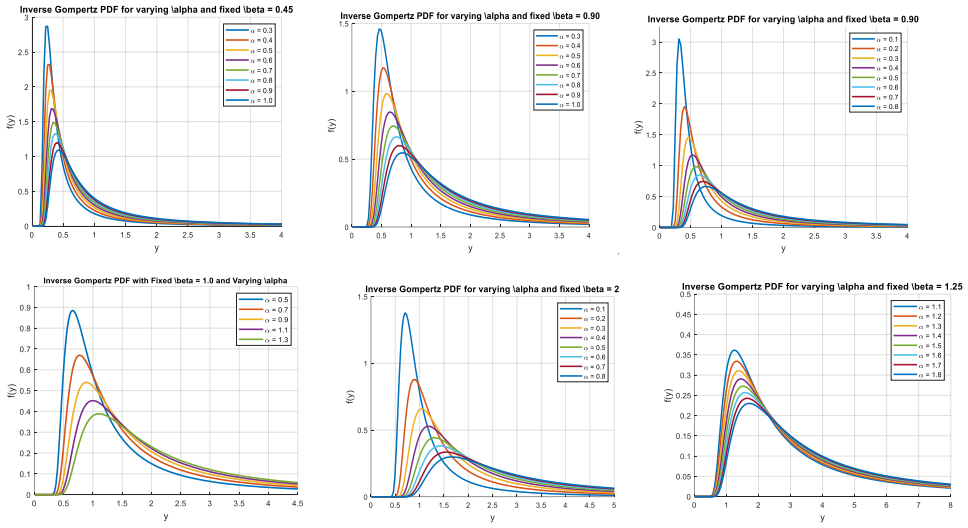


Fig. 1. Inverse Gompertz Distribution: Behaviour of PDF Under Varying Shape Parameters α and β.

I.i. Survival and risk function

Survival analysis is a basic statistical model that has been used in a wide range of fields, such as medicine, biology, social sciences, econometrics, and engineering. Its approach revolves around the examination of the time of events, usually over a long period that cuts across a number of years. Informally, the time-to-event analysis sometimes has been called survival analysis, which considers how survival time is distributed (and the determinants of this distribution). This is the main variable, which is the period between the well-defined beginning (which may be birth or the beginning of treatment) and the end (which may be death or treatment failure). By definition, later or repeat outcomes that fail to satisfy the condition of terminal events are outside the parameters of this framework [XX-XXVIII]. Survival analysis is fundamentally based on the amount of content, the survival function, which is a statement of the probability that survival time will be greater than a given value, in the region. It stands for the probability of an individual or unit of study continuing after a specific time barrier. This operation supports a lot of theoretical and practical research in the field of survival analysis, which provides important information about the risk patterns, efficacy of treatment, and long-term results of various fields of science [I-XII].

$$S(y|\alpha,\beta) = \Pr(Y > y) = 1 - F(y|\alpha,\beta),$$
$$= 1 - \exp\left[-\alpha\left(e^{\frac{\beta}{y}} - 1\right)\right];\ y > 0. \qquad (3)$$

S (t) is a diminishing function, and it plays decreasingly compared to t because it starts from 1 and it tends to zero when t tends to infinity. The basic rationale of this feature is that the survival probability decreases in time.

Figure 2 (a-f) displays the survival function curves, which exhibit varied shape-scales in the Inverse Gompertz distribution. Figure 3 provides a graphical representation of the $S(t)$ and $f(t)$ of the three-dimensional nature. The graphic Visualization gives us knowledge of how the probability and duration of survival interact with parameters and time under the Inverse Gompertz distribution.

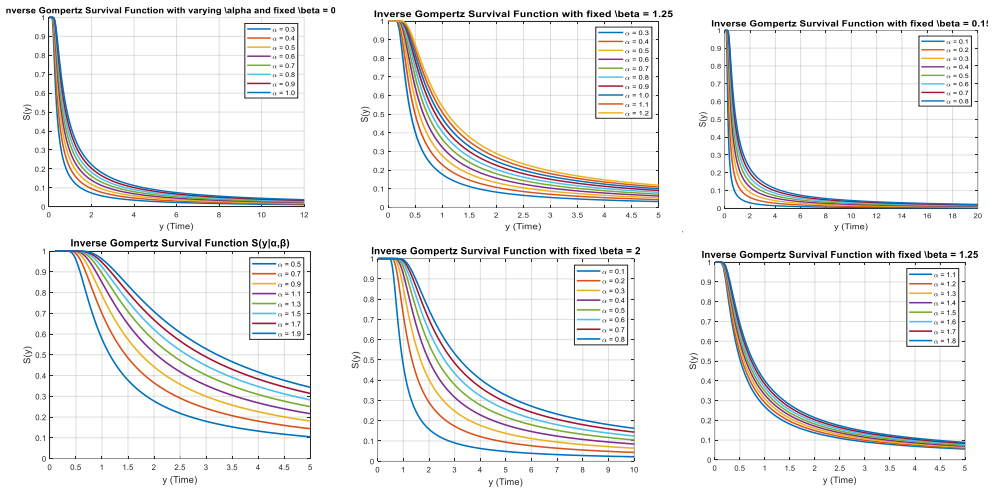


Fig. 2. Inverse Gompertz Distribution: Behaviour of SF Under Varying Shape Parameters α and β.

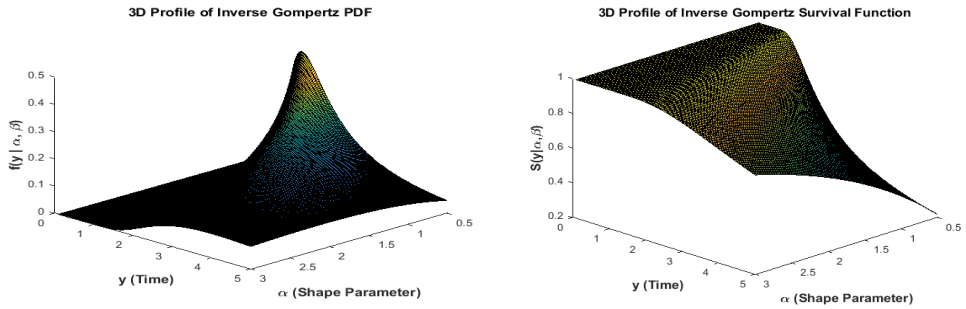


Fig. 3. 3D Plots of PDF and Survival Function

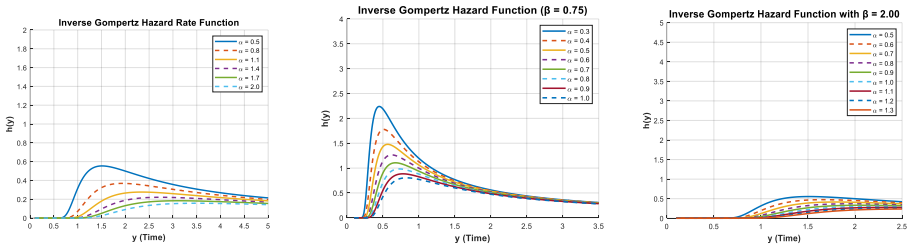
The hazard rate function, commonly known by statisticians as the instantaneous failure rate, is a key concept in survival analysis. It measures the probability of failure at any point in time, given the probability of surviving to the time point t. Hazard functions are especially significant in biomedical research because they determine the possibility of patients experiencing a phenomenon or event, whether death or recurrence of the disease, within a particular time period after they have attained that point in time. Equally, in reliability engineering, hazard rates are the essential capture of the natural propensity of elements or systems to degrade in their existence. Mathematically, the hazard rate is mathematically defined as follows [V, XX-XXX]:

$$h(y) = \frac{f(y)}{S(y)}, \tag{4}$$

The hazard rate function (HRF) of the Inverse Gompertz distribution.

$$h(y;\alpha,\beta) = \frac{\frac{\alpha\beta}{y^2}\exp\left(\frac{\beta}{y}\right)\exp\left[-\alpha\left(e^{\frac{\beta}{y}}-1\right)\right]}{1-\exp\left[-\alpha\left(e^{\frac{\beta}{y}}-1\right)\right]};\ \ y>0. \tag{5}$$

Figures 4 and 5 give illustrative profiles of the hazard rate function (HRF). All these profiles have unique shapes, such as decreasing, unimodal, and hump-shaped, all of which give useful flexibility in the lifetime modelling. This functional diversity would be of particular benefit in real-world reliability and survival studies because the HRF can model simple monotonic trends, but also more complex and multifaceted hazard trends that often appear in empirical data.



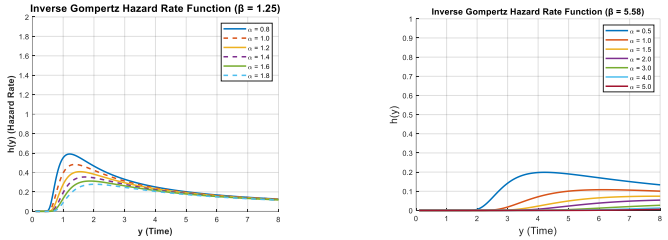


Fig. 4. Features of α and β on HRF

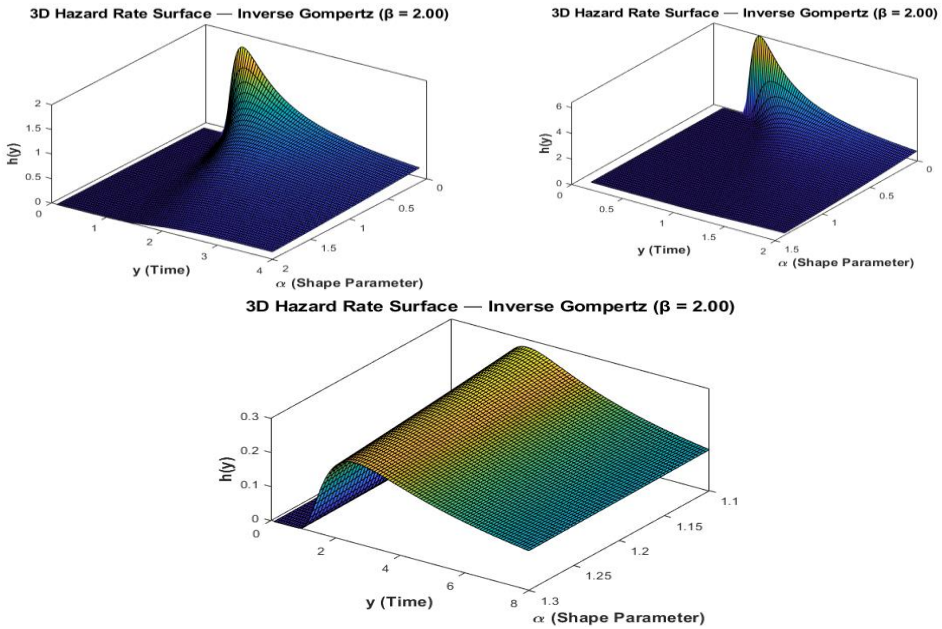


Fig. 5. 3D profile of HRF of Inverse Gompertz distribution

The cumulative hazard rate function (CHRF) is a key concept in survival analysis because it is used to measure the cumulative amount of risk that subjects have incurred since the beginning of the observation period until a specified time t. Denoted as $F'(y|\alpha,\beta)$, the CHRF gives a holistic account of risk exposure with time. The CHRF is especially useful in the framework of the Inverse Gompertz distribution that shows the dynamics of the risk accumulation process and provides completeness to the data expressed by the hazard and survival functions. A combination of these functions provides a consistent system for describing the lifetime behaviour and comprehending the mechanisms of failure processes.

$$F'(y|\alpha,\beta) = \int_0^t h(y|\,\alpha,\beta)\,ds = -\log\left[1-\exp\left[-\alpha\left(e^{\frac{\beta}{y}}-1\right)\right]\right]. \tag{6}$$

In the case of the Inverse Gompertz distribution, the CHRF follows an even accelerating trend showing the gradual increase in risk with age. This positive curvature has been representative of trends that are often found in both survival analysis and reliability analysis, when risk increases with time of exposure.

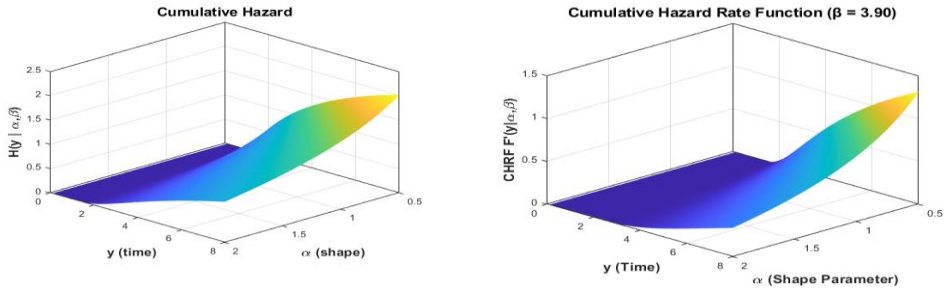


Fig. 6. Features of α and β on CHRF

A random variable that is the lifetime duration is correlated with a reverse hazard rate function (RHRF), which is defined when the ratio of the cumulative distribution function to a probability density function is available. The RHRF mathematically defines the probability of failure at time given that the event has already occurred before time. This operation is pivotal in left-censored analysis and is thus important, especially in fields of forensic science, actuarial science, and early failure. The survival time-based reliability function. The RHRF can be successful in analysing systems that tend to fail during the initial observation period. Additional reasons supporting the significance of reliability theory and stochastic models are research findings indicating that the RHRF plays a role in the distribution characterization, the creation of diagnostic checks, and the creation of novel reliability models [XXX-XLVIII]. Figure 7 mathematical foundations and applications and general use) gives a graphical representation of these concepts.

$$h'(y;\alpha,\beta) = \frac{\alpha\beta}{y^2}\exp\left(\frac{\beta}{y}\right). \tag{7}$$

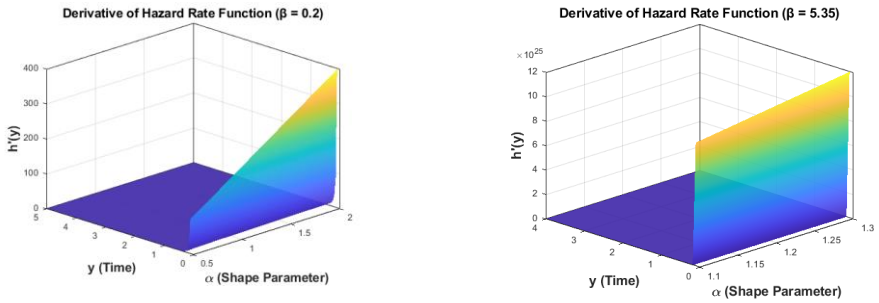


Fig. 7. Features of α and β on RHRF

As shown in Figure 8, it is an effective tool of analysis in reliability and durability research because of its intrinsic relationship with the hazard (failure) rate. This metric is important in survival analysis by highlighting the actions of the distributional tail, especially in determining the performance of systems and the dynamics of risk over their existence periods.

$$MR(y;\alpha,\beta) = \frac{y^2}{\alpha\beta}\left(e^{\alpha(e^{\beta/y}-1)-\beta/y} - e^{-\beta/y}\right). \tag{8}$$

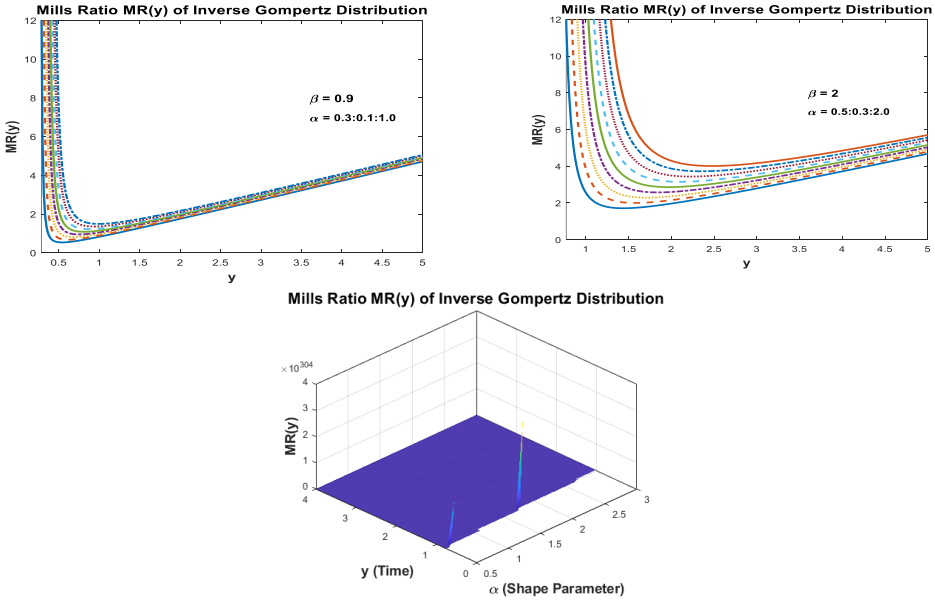


Fig. 8. Features of α and β on MR.

The $OF(y|\alpha,\beta) = \frac{F(y|\alpha,\beta)}{S(y|\alpha,\beta)}$ is

$$OF(y|\alpha,\beta) = \frac{\exp\left[-\alpha\left(e^{\frac{\beta}{y}}-1\right)\right]}{1-\exp\left[-\alpha\left(e^{\frac{\beta}{y}}-1\right)\right]}. \quad (9)$$

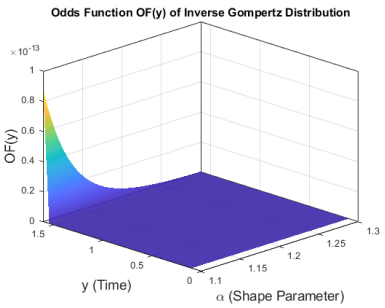


Fig. 9. Features of α and β on OF

II. Estimation methods

II.i. Maximum likelihood estimation

The parameters of the Inverse Gompertz distribution are estimated using the Maximum Likelihood Estimation (MLE) method. Let $t_1, t_2, \ldots, t_n$. denote an independent random sample from the Inverse Gompertz distribution. The likelihood function is constructed from the probability density function and maximized numerically to obtain parameter estimates. For brevity, the complete derivations of the log-likelihood function, score equations, and information matrix are provided in Appendix A.

II.ii. Handling of Right-Censored Survival Data

Although the datasets analysed in this study contain only fully observed survival times, many clinical survival studies include right-censored observations due to loss to follow-up or the termination of the study before the occurrence of the event of interest. In the presence of censoring, the likelihood function must incorporate contributions from both observed events and censored observations. Let y_i denote the observed survival time and let δ_i be the event indicator defined as

$$\delta_i = \begin{cases} 1, & \text{if the event time is observed} \\ 0, & \text{if the observation is right-censored.} \end{cases}$$

The likelihood function for censored survival data is therefore expressed as

$$L(\alpha, \beta) = \prod_{i=1}^{n} f(y_i)^{\delta_i} S(y_i)^{1-\delta_i}, \tag{10}$$

where $f(y_i)$ is the probability density function and $S(y_i)$ is the survival function of the Inverse Gompertz distribution. This formulation allows censored observations to contribute information through the survival function. Within the proposed IG-SVM framework, the machine learning component could also be extended to censored settings by training the regression model using censoring-adjusted loss functions or inverse-probability weighting schemes. Such extensions would enable the proposed methodology to be applied to more general survival datasets where incomplete follow-up is present.

II.iii. Estimation of Reliability-Oriented Survival Functions

The survival function is estimated, which is later used in the general log-likelihood expression, as follows:

$$l(\mathrm{y}|\alpha, \beta) = n! \prod_{i=1}^{n} S(y_i|\alpha, \beta) = \mathrm{n!} \prod_{\mathrm{i=1}}^{\mathrm{n}} \left(1 - \exp\left[-\alpha\left(e^{\frac{\beta}{y_i}} - 1\right)\right]\right), \tag{11}$$

Because of the ease of algebraic manipulation of the log-likelihood, the natural logarithm of the likelihood function is analysed (Equation 10). Its exponential case gives the following representation of its log-likelihood:

$$\ln l(\mathrm{y}|\alpha, \beta) = \ln n! + \sum_{i=1}^{n} \ln\left(1 - \exp\left[-\alpha\left(e^{\frac{\beta}{y_i}} - 1\right)\right]\right). \tag{12}$$

Then $\frac{\partial \ln l\,(.)}{\partial(.)}\, w.r.t.\, \alpha$ and β are:

$$\frac{\partial \ln l(\mathrm{y}|\alpha,\beta)}{\partial \alpha} = -\sum_{i=1}^{n} \frac{e^{\frac{\beta}{y_i}-1}}{\exp\left[-\alpha\left(e^{\frac{\beta}{y_i}-1}\right)\right]-1}, \tag{13}$$

$$\frac{\partial \ln l(\mathrm{y}|\alpha,\beta)}{\partial \beta} = -\sum_{i=1}^{n} \frac{\alpha \exp\left[-\alpha\left(e^{\frac{\beta}{y_i}-1}\right)\right]}{1-\exp\left[-\alpha\left(e^{\frac{\beta}{y_i}-1}\right)\right]} \cdot \frac{e^{\frac{\beta}{y_i}}}{y_i} \tag{14}$$

II.iv. Modified Support Vector Machine

The Support Vector Machine regression (SVR) in this study serves as a surrogate modelling tool to estimate the reliability-oriented survival functionals implied by the Inverse Gompertz (IG) distribution. In this model, the IG parameters (alpha, beta) are estimated by first performing Maximum Likelihood Estimation (MLE). Then, SVR is trained to understand the mapping between the survival time t and the IG based outputs: the probability density function f(t), the survival function S(t), and the hazard rate h(t). This design allows a direct comparison between (i) the analytical parametric estimates based on the fitted IG model and (ii) the data-based functional approximations based on the SVR, based on predictive accuracy measures (e.g., RMSE). We use the Radial Basis Function (RBF) kernel to represent potential nonlinearities; the RBF kernel is generally useful in nonlinear regression problems. Hyperparameters such as the regularization parameter C of the SVR and the coefficient of the kernel γ-are chosen using grid search with 10 -fold cross-validation, whereby the minimum validation RMSE is used. Input times are all normalized (zero means, unit variance) to enhance numerical stability and convergence t.

Algorithm 1: IG-SVR Surrogate Modelling for Reliability Functionals

XL. Observed survival times

SVR predictors $\hat{f}(t), \hat{S}(t), \hat{h}(t)$ and error metrics

1. Fit parametric baseline (IG via MLE). Estimate ($\hat{\alpha}, \hat{\beta}$) by maximizing the IG likelihood based on $\{t_i\}_{i=1}^{n}$.
2. Generate training targets (IG functionals). $i = 1$ to n Compute IGbased targets using $(\hat{\alpha}, \hat{\beta})$:

$y_i^{(f)} = f(t_i; \hat{\alpha}, \hat{\beta}), y_i^{(S)} = S(t_i; \hat{\alpha}, \hat{\beta}), y_i^{(h)} = h(t_i; \hat{\alpha}, \hat{\beta})$.

3. Preprocess inputs.

Standardize times to $\tilde{t}_i = (t_i - \bar{t})/s_t$.

4. Train SVR models (one per functional).

Train separate SVR regressors to learn
$\tilde{t} \mapsto y^{(f)}, \tilde{t} \mapsto y^{(S)}, \tilde{t} \mapsto y^{(h)}$.
Use an RBF kernel and tune (C, γ) via grid search with 10 -fold cross-validation, minimizing RMSE.

5. Validation and performance evaluation.

On held-out folds, compute predictions $\hat{f}(t), \hat{S}(t), \hat{h}(t)$ and evaluate

$$\text{RMSE} = \sqrt{\frac{1}{m}\sum_{j=1}^{m}\left(\hat{g}(t_j) - g(t_j; \hat{\alpha}, \hat{\beta})\right)^2}$$

where $g \in \{f, S, h\}$ and m is the number of validation points. The flowchart of the SVM pipeline is given, which reports the data preprocessing phase, the model training and hyperparameter optimization, and the prediction process.

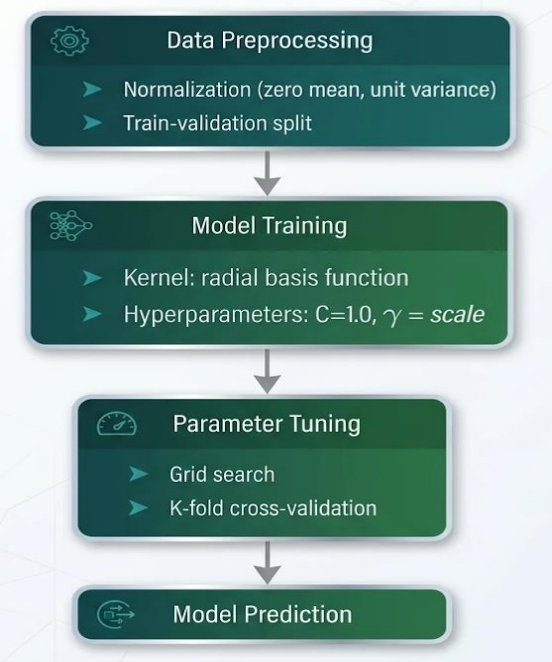


Fig. 10. The SVM pipeline flowchart.

Figure 10 is a workflow that shows the consecutive steps of the suggested SVM-based modelling framework. The initial step is the standardization of the raw survival data before it is used to make the data numerically stable and scale uniformly across cases. This data is further split into training and validation sets to enable the process of model learning and evaluation of model performance.

1. The Support Vector Machine regression model is then trained on the training dataset in the second stage. In this stage, the algorithm gets to learn the functional relationship between the observed survival times and the quantities that are related to reliability obtained via the Inverse Gompertz distribution. The choice of the kernel function depends on the learning process, which allows the model to elicit possible nonlinear relations among the survival data.

2. The third step is the hyperparameter optimization. A grid search algorithm with cross-validation is applied in order to find the best values of the regularization parameter and the kernel coefficient that best minimize the error in prediction.

3. Lastly, during the validation step, the trained model is tested on the validation data. The model predictive power is evaluated by means of the Root Mean Square Error (RMSE) and other performance indicators, which enables one to make a comparative analysis of the SVM-based predictions with the estimates received with the help of the classical Maximum Likelihood Estimation method.

II.v. Role of SVM in the IG–SVM Framework

Two possible interpretations arise when combining machine learning with parametric survival models. In the first interpretation, the machine learning model is used purely as a predictive surrogate that approximates survival functionals and probability density.

In the second interpretation, the machine learning model directly assists in estimating the distribution parameters. In this study, the first interpretation is adopted. The Support Vector Machine (SVM) model is used purely as a predictive approximation tool for reliability functionals derived from the Inverse Gompertz distribution. The parameters (α, β) of the Inverse Gompertz model are estimated using the Maximum Likelihood Estimation (MLE) method, while the SVM model is trained to approximate the corresponding survival-related functions based on the observed time-to-event data. Under this framework, the comparison between MLE and SVM focuses on the predictive accuracy of estimated survival quantities rather than on direct parameter estimation. Specifically, the SVM model approximates the mapping

$$t \to \{f(t), S(t), h(t)\}, \tag{15}$$

where $f(t)$ denotes the probability density function, $S(t)$ denotes the survival function, and $h(t)$ denotes the hazard rate. The predictive performance of the two approaches is evaluated using Root Mean Square Error (RMSE) and related accuracy measures. This specification retains the parametric structure of the Inverse Gompertz model, but allows the machine learning model to give a flexible nonparametric estimation of the survival dynamics.

V. Simulation

Simulation is a methodology related to the process of reproducing real systems in an experimental controlled environment in an effort to study the behavior of the system. The main aim is to construct an artificial model of a process which repeats the principal actions of the real system in the given conditions. This necessitates a simpler but representative model, which on one side we have the structural qualities and alternatively the main operation of the whole system. The surrogate model can be experimentally verified, and the experimental results can be used to provide knowledge that can be applied to the actual system. Simulation: When used computationally, simulation is the construction and running of mathematical programs that imitate actual programming contexts. Such simulations are used to repeatedly run them to view and evaluate the outcomes, so that statistically acceptable conclusions regarding the performance and behavior of the system under uncertainty may be made [XLII].

The popular simulation techniques are the Monte Carlo methodology, the analog technique, and the mixed technique. The most prominent one is the Monte Carlo simulation, which uses probabilistic sampling techniques to simulate difficult phenomena under a known probability distribution. In this procedure, one needs to create a cumulative distribution function (CDF) from which independent and identically distributed random samples are generated. All observations are processed one by one in a sequence by suitable mathematical methods to provide statistical validity and replicability. In this study, the performance of the proposed estimators of the Inverse Gompertz distribution when it is fuzzy was investigated using simulation, thereby simplifying the formulation of theoretical constructs and practical usage of the theory. The proposed estimation methods were empirically verified in a structured simulation context. The accuracy of the estimators for different sample sizes was evaluated by the Root Mean Square Error (RMSE) criterion, which gives insight into the relative accuracy of the estimators. The simulator design therefore makes it possible to perform a comparative evaluation of the proposed approaches on several data

scenarios that mirror real-world scenarios. The approach provided here gives the most reliable and efficient functional estimation of the Inverse Gompertz distribution. The proposed approach enhances the decision-making process [I-XX].

- Change in sample size.
- Change in model parameter values.

Stage I: Model Setup and Parameter Configuration

A first step is basic as it forms the framework for all later simulation methods. At this stage, the parametric values are set, the main hypotheses are given, and the behavior of the whole process is described. This phase is composed of three sequential parts:

Step 1: The first step of the procedure involves selecting the default parameter values

Simulation parameter settings should be reported to ensure reproducibility. For each scenario, the true values of the IG parameters, the number of independent replications, the seed for the random numbers, and the data-generation technique should be supplied. The sample sizes in the publication are 50, 100, 500, and 1,000 replications; the parameter values should be validated against the simulation code and tables.

Step 2: Sample Size Specification

During the simulation, the stability and the performance of the estimators were examined using different sample sizes, which comprised small, medium, and large sets of data.

- n =50;100;500;1000.

Stage II: Random Data Simulation through Inverse Transformation

For each replication, the sample should be divided into training and validation parts with the same partitions for the approaches to be compared. All pre-processing and hyperparameter selection must be done on training data only. - Observations for validation shall not be used for parameter estimation, target construction, or tuning. Fold-level errors should be averaged over folds and replications, and variability should be described by standard errors or confidence intervals. Summing fold scores is not an interpretable average performance indicator.

Step 1. Uniform Random Variable Generation

$$\text{Let } u_i \sim U(0,1), i = 0,1,2,\dots,n. \tag{16}$$

At this point, the default $rand$ function of MATLAB is used to create independent and identically distributed $(i.i.d.)$ random variables of the uniform distribution on the interval (0,1). The official statement is as follows:

Step 2: Transformation to Inverse Gompertz Distributed Data

The uniform random variables so generated are then converted to observations using the function of the Inverse Gompertz process, which involves the inverse cumulative distribution (CDF). In this work, the inverse mapping and the well-known CDF of the Inverse Gompertz distribution, as in Equation (1), are used in this transformation $x_i = F^{-1}(y)$, This procedure simplifies to:

$$Y_i = \frac{\beta}{\ln\left(1-\frac{\ln U}{\alpha}\right)}, U \sim U(0,1), i = 0,1,2,\dots,n. \quad (17)$$

The last performance measure was the average of all folds RMSE values, which provides a more generalized and statistically significant estimate of model performance.

Step 3: Algorithm for Generating Inverse Gompertz Random Variables

1. Specify parameters $\alpha > 0$ and $\beta > 0$.
2. Generate $U_i \sim \text{Uniform}(0,1)$.
3. Compute simulated observation $Y_i = \frac{\beta}{\ln\left(1-\frac{\ln U_i}{\alpha}\right)}$.

Repeat steps $2-3$ until the desired sample size n is obtained

Step 3: **Matched Cross-Validation Evaluation Protocol**

The manuscript describes 10-fold cross-validation. To avoid information leakage, splitting must occur before fitting the IG distribution and before generating SVR targets. Within each training fold, fit the IG parameters and construct the corresponding functional targets; then fit SVR and evaluate both approaches on the untouched validation fold. If SVR was trained on targets generated using parameters estimated from the full dataset, the reported validation error is optimistic and must be recalculated.

1. The k^{th} fold was held out as the validation set.
2. The remaining K-1 folds were used as the training set.
3. The MLE method was fitted using only the training folds to obtain the parameter estimates of the Inverse Gompertz distribution.
4. The SVM regression model was trained on the same training folds using the optimized hyperparameters obtained from the grid search procedure.
5. Both fitted models were then evaluated on the held-out fold using the Root Mean Square Error (RMSE) and other predictive performance metrics.

Performance should be précised as a mean fold-level metric, not the sum of fold scores. Because SVR is trained to reproduce IG-derived targets, its RMSE should be labelled surrogate approximation error. It is not directly comparable with sampling error or goodness-of-fit of MLE unless both methods are evaluated against a common, independently defined reference target.

$$\bar{M} = \frac{1}{K}\sum_{k=1}^{K} M_k \quad (18)$$

The performance variability of the estimates of the performance was measured by calculating the standard error between folds.

Stage III: Parameter Estimation

The parametric estimation stage estimates the IG distribution by maximum likelihood. The SVR step is a separate approximation stage mapping normalized time to selected IG-derived functionals. As the outputs are continuous, the manuscript should

constantly use support vector regression (SVR), rather than classification-oriented SVM.

- Maximum Likelihood Estimations.
- Modified Support Vector Machine.

RMSE alone should not be used for model selection. Goodness-of-fit should be measured by the loglikelihood, AIC, AICc/CAIC (and an exact definition of this should be supplied), BIC, and graphical diagnostics. The predictive assessment requires an independent validation design and a well-defined target population.

Stage IV: Experiment is repeated (1000) times.

Stage V: Compute the perfuses.

$$RMS(\hat{\alpha}) = \sqrt{\frac{\sum_{i=1}^{Q}(\widehat{\alpha_i}-\alpha_i)^2}{Q}}, \tag{19}$$

$$RMS(\hat{\beta}) = \sqrt{\frac{\sum_{i=1}^{Q}(\widehat{\beta_i}-\beta_i)^2}{Q}}. \tag{20}$$

Table 1: RMSE of Survival Function Estimates Under Different Parameter Settings, Methods, and Sample Sizes.

Parameters	Sample Size (n)	Methods							
		MLE				SVM			
		$\hat{\alpha}$	$\hat{\beta}$	$\hat{s}(t)$	Abs. Bias	$\hat{\alpha}$	$\hat{\beta}$	$\hat{s}(t)$	Abs. Bias
$\alpha = 0.2; \beta = 2.0$	50	0.214	1.97	0.0123	0.0081	0.225	1.95	0.0154	0.0103
	100	0.207	1.99	0.0086	0.0054	0.214	1.97	0.0098	0.0061
	500	0.203	2.01	0.0031	0.0022	0.206	1.99	0.0042	0.0029
	1000	0.201	2.00	0.0017	0.0011	0.203	2.00	0.0021	0.0014
$\alpha = 2.5; \beta = 2.5$	50	2.47	2.53	0.0146	0.0094	2.41	2.57	0.0182	0.0121
	100	2.49	2.51	0.0102	0.0063	2.46	2.54	0.0113	0.0075
	500	2.50	2.50	0.0041	0.0021	2.48	2.52	0.0052	0.0031
	1000	2.50	2.50	0.0023	0.0010	2.49	2.51	0.0028	0.0015
$\alpha = 2.7; \beta = 4.6$	50	2.66	4.72	0.0184	0.0113	2.62	4.78	0.0226	0.0144
	100	2.69	4.67	0.0125	0.0072	2.66	4.71	0.0151	0.0092
	500	2.70	4.61	0.0053	0.0031	2.68	4.64	0.0068	0.0038
	1000	2.70	4.60	0.0027	0.0015	2.69	4.61	0.0032	0.0019
$\alpha = 3.0; \beta = 5.3$	50	2.91	5.41	0.0203	0.0131	2.86	5.48	0.0247	0.0158
	100	2.95	5.36	0.0142	0.0085	2.91	5.41	0.0172	0.0101
	500	2.98	5.31	0.0064	0.0036	2.95	5.35	0.0078	0.0044
	1000	2.99	5.30	0.0030	0.0017	2.97	5.32	0.0039	0.0021

Table 2: RMSE Analysis of Hazard Function Prediction Across.

Parameters	Sample Size (n)	Methods							
		MLE				SVM			
		$\hat{\alpha}$	$\hat{\beta}$	$\hat{h}(t)$	Abs. Bias	$\hat{\alpha}$	$\hat{\beta}$	$\hat{h}(t)$	Abs. Bias
	50	0.214	1.97	0.0182	0.0104	0.225	1.95	0.0217	0.0133
	100	0.207	1.99	0.0126	0.0072	0.214	1.97	0.0145	0.0084
	500	0.203	2.01	0.0051	0.0031	0.206	1.99	0.0064	0.0039

$\alpha = 0.2; \beta = 2.0$	1000	0.201	2.00	0.0028	0.0016	0.203	2.00	0.0032	0.0020
$\alpha = 2.5; \beta = 2.5$	50	2.47	2.53	0.0201	0.0126	2.41	2.57	0.0238	0.0147
	100	2.49	2.51	0.0142	0.0081	2.46	2.54	0.0166	0.0098
	500	2.50	2.50	0.0062	0.0034	2.48	2.52	0.0075	0.0042
	1000	2.50	2.50	0.0035	0.0019	2.49	2.51	0.0039	0.0022
$\alpha = 2.7; \beta = 4.6$	50	2.66	4.72	0.0223	0.0141	2.62	4.78	0.0257	0.0163
	100	2.69	4.67	0.0156	0.0092	2.66	4.71	0.0184	0.0108
	500	2.70	4.61	0.0068	0.0039	2.68	4.64	0.0083	0.0047
	1000	2.70	4.60	0.0036	0.0021	2.69	4.61	0.0042	0.0025
$\alpha = 3.0; \beta = 5.3$	50	2.91	5.41	0.0246	0.0157	2.86	5.48	0.0282	0.0184
	100	2.95	5.36	0.0171	0.0103	2.91	5.41	0.0197	0.0119
	500	2.98	5.31	0.0076	0.0044	2.95	5.35	0.0089	0.0051
	1000	2.99	5.30	0.0039	0.0023	2.97	5.32	0.0046	0.0027

Table 3. RMSE of PDF Prediction Under Different Parameter Settings, Methods, and Sample Sizes.

Parameters	Sample Size (n)	Methods							
		MLE				SVM			
		$\hat{\alpha}$	$\hat{\beta}$	$\hat{f}(t)$	Abs. Bias	$\hat{\alpha}$	$\hat{\beta}$	$\hat{f}(t)$	Abs. Bias
$\alpha = 0.2; \beta = 2.0$	50	0.214	1.97	0.0176	0.0103	0.225	1.95	0.0208	0.0128
	100	0.207	1.99	0.0124	0.0071	0.214	1.97	0.0143	0.0083
	500	0.203	2.01	0.0052	0.0030	0.206	1.99	0.0065	0.0037
	1000	0.201	2.00	0.0027	0.0016	0.203	2.00	0.0033	0.0019
$\alpha = 2.5; \beta = 2.5$	50	2.47	2.53	0.0194	0.0121	2.41	2.57	0.0227	0.0142
	100	2.49	2.51	0.0136	0.0079	2.46	2.54	0.0161	0.0096
	500	2.50	2.50	0.0060	0.0033	2.48	2.52	0.0073	0.0040
	1000	2.50	2.50	0.0032	0.0018	2.49	2.51	0.0038	0.0021
$\alpha = 2.7; \beta = 4.6$	50	2.66	4.72	0.0218	0.0139	2.62	4.78	0.0253	0.0161
	100	2.69	4.67	0.0154	0.0091	2.66	4.71	0.0181	0.0106
	500	2.70	4.61	0.0067	0.0038	2.68	4.64	0.0081	0.0045
	1000	2.70	4.60	0.0034	0.0020	2.69	4.61	0.0040	0.0024
$\alpha = 3.0; \beta = 5.3$	50	2.91	5.41	0.0237	0.0152	2.86	5.48	0.0274	0.0176
	100	2.95	5.36	0.0168	0.0101	2.91	5.41	0.0192	0.0116
	500	2.98	5.31	0.0074	0.0042	2.95	5.35	0.0086	0.0049
	1000	2.99	5.30	0.0037	0.0022	2.97	5.32	0.0043	0.0026

VI. Numerical Example

The numerical comparison should distinguish probability-based goodness of fit from approximation error. AIC and BIC are based on similar likelihoods, and penalize the complexity of the model. The RMSE is meaningful only if the reference values and evaluation points are reliably defined. Provide the specific formula and aim for each statistic given.

$$AIC = 2n_1 - 2\ln(L), \tag{21}$$

$$CAIC = AIC + 2\frac{n_2(n_2+1)}{n_1-n_2-1}, \tag{22}$$

$$BIC = n_1\ln(n_2) - 2\ln(L). \tag{23}$$

Vi.i. Dataset I

Dataset I: 50 breast-cancer patients treated in Medical City Hospital, Baghdad, during 2020. The recording interval is described inconsistently as admission-to-discharge and as a survival time terminating in death. Authors must check the exact time origin, event definition, units, and inclusion criteria before publication. Discharge status alone should not be used to confirm death without source record confirmation.

VI.i.a. Handling of Censoring in Survival Data

The manuscript treats both cohorts as complete, uncensored event-time samples and therefore uses a density-based likelihood. This assumption requires verification for every observation. If a patient was alive at last contact, lost to follow-up, or otherwise had an incomplete event time, that observation is right-censored and must contribute to the survival function rather than the density. For observed time t_i and event indicator δ_i, the likelihood contribution is $f(t_i)_i^{\delta} S(t_i)^{1-\delta_i}$. The complete-case analysis cannot be generalized to censored survival settings.

VI.i.b. Goodness of-fit tests for data set

Where appropriate, goodness of fit should be checked on the original time scale using empirical distribution plots, fitted density and survival curves, probability plots and formal tests. A straight-line pattern on a transformed plot is merely a diagnostic and does not prove the IG distribution to be true. The transformation and plotting positions are to be given.

$$\ln[S(y)] = \ln\left(1 - \exp\left[-\alpha\left(e^{\frac{\beta}{y}} - 1\right)\right]\right). \tag{24}$$

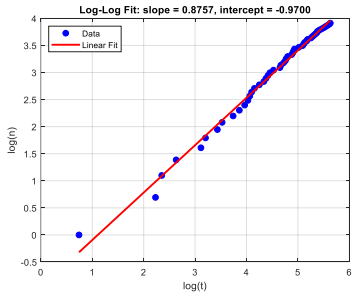


Fig. 11. For Dataset I, the logarithm of the cumulative data volume is expressed in distributive form.

VI.i.c. Results

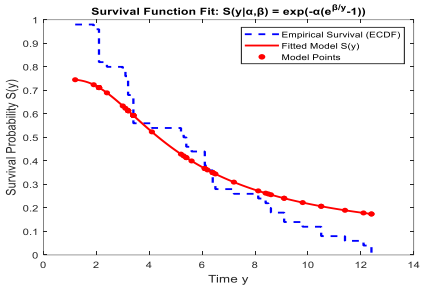
Table 4 contains the estimates of the model parameters. Table 5 provides the model estimation methodology compared to the criteria of the RMSE.

Table 4: Presents the estimated parameter values of the Inverse Gompertz distribution

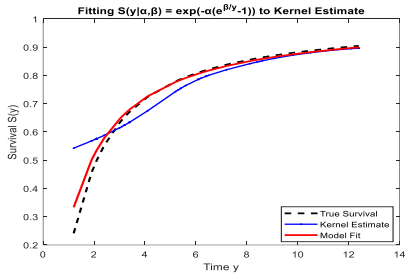
Methods	Parameters			
	$\hat{\alpha}_{MLE}$	$\hat{\beta}_{MLE}$	$\hat{\alpha}_{SVM}$	$\hat{\beta}_{SVM}$
Survival	0.5766	3.2069	0.464956	4.028335
Risk function	0.015749	36.713686	0.16445	1.84851
Probability density function	51.132010	0.010257	0.211720	0.00062

Table 5: Estimated S(t) and h(t) at Observed Time Points (Application Data).

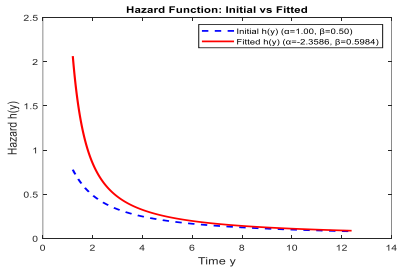
t_i	$\hat{S}(t)_{MLE}$	$\hat{S}(t)_{SVM}$	$\hat{h}(t)_{MLE}$	$\hat{h}(t)_{SVM}$	t_i	$\hat{S}(t)_{MLE}$	$\hat{S}(t)_{SVM}$	$\hat{h}(t)_{MLE}$	$\hat{h}(t)_{SVM}$
1.9	0.0014	3.35E-05	0.0108	0.0104	5.4	0.0074	1.29E-05	0.0891	0.0005
2.1	0.0030	6.27E-05	0.2540	0.0072	5.6	0.0064	1.03E-05	0.0856	0.0006
2.1	0.0030	6.27E-05	0.2540	0.0072	6.1	0.0026	5.27E-06	0.0778	0.0011
2.1	0.0030	6.27E-05	0.2540	0.0072	6.1	0.0026	5.27E-06	0.0778	0.0011
2.1	0.0030	6.27E-05	0.2540	0.0072	6.1	0.0026	5.27E-06	0.0778	0.0011
2.1	0.0030	6.27E-05	0.2540	0.0072	6.2	0.0013	3.80E-06	0.0736	0.0012
2.1	0.0030	6.27E-05	0.2540	0.0072	6.4	0.0001	3.35E-06	0.0736	0.0015
2.1	0.0030	6.27E-05	0.2540	0.0072	6.4	0.0001	3.35E-06	0.0736	0.0015
2.4	2.46E-06	4.56E-05	0.2217	0.0029	6.4	0.0001	3.35E-06	0.0736	0.0015
3	0.0125	3.05E-07	0.1685	0.0001	6.5	0.0007	3.43E-06	0.0724	0.0016
3.1	0.0124	2.19E-06	0.1627	6.86E-5	7.2	0.0002	7.55E-06	0.0643	0.0025
3.2	0.0024	6.52E-06	0.1573	1.02E-5	8.12	1.3E-05	1.02E-05	0.0559	0.0031
3.2	0.0024	6.52E-06	0.1573	1.02E-5	8.4	0.0002	8.77E-06	0.0537	0.0030
3.2	0.0024	6.52E-06	0.1573	1.02E-5	8.5	0.0010	8.50E-06	0.0530	0.0020
3.2	0.0024	6.52E-06	0.1573	1.02E-5	8.6	0.0024	8.19E-06	0.0522	0.0028
3.4	0.0012	1.52E-05	0.1475	2.03E-5	9.1	0.0058	6.12E-06	0.0488	0.0021
3.4	0.0012	1.52E-05	0.1475	2.03E-5	9.1	0.0058	6.12E-06	0.0488	0.0021
3.4	0.0012	1.52E-05	0.1475	2.03E-5	9.8	0.0064	1.13E-06	0.0446	0.0007
3.4	0.0012	1.52E-05	0.1475	2.03E-5	10.5	0.0112	1.12E-06	0.0410	2.78E-6
3.4	0.0012	1.52E-05	0.1475	2.03E-5	10.5	0.0112	1.12E-06	0.0410	2.78E-6
3.4	0.0012	1.52E-05	0.1475	2.03E-5	11.4	0.0122	4.02E-06	0.0369	0.0022
4.1	0.0019	1.63E-05	0.1206	0.0002	12.1	0.0145	2.06E-07	0.4326	0.0092
5.2	0.0173	1.46E-05	0.1020	0.0004	12.4	0.0244	8.25E-08	0.0331	0.0142
5.3	0.0141	1.39E-05	0.1110	0.0005	12.4	0.0244	8.25E-08	0.0331	0.0142



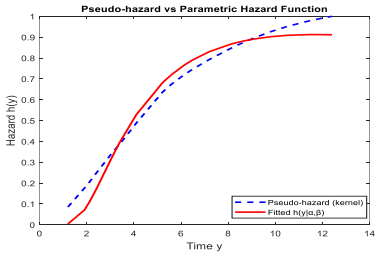
(a) Survival by MLE



(b) Survival by SVM



(c) Hazard by MLE



(d) Hazard by SVM

Fig. 12. Comparative Analysis of Survival and Hazard Function Estimation Using MLE and SVM Methods.

The survival function must be non-increasing and bounded between zero and one. The hazard function is not necessarily to be monotonically increasing; its shape is

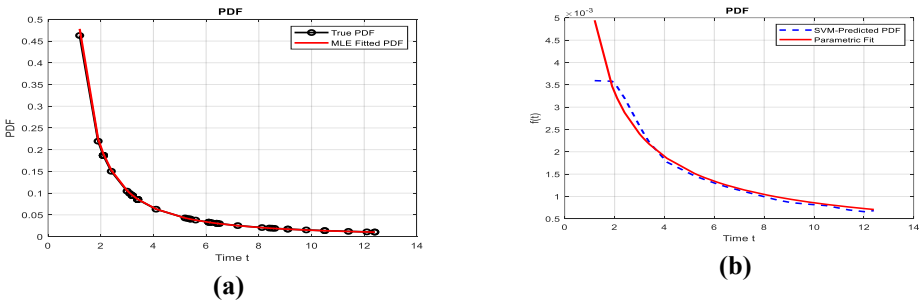
determined by the fitted distribution and should be described from the estimated curve itself. The hazard should not be described as monotonically growing and unimodal in the text. Clinical interpretation should remain descriptive as the current models do not include age, tumor stage, therapy, comorbidities, or other patient-level factors.

VI.i.d.1. Clinical Interpretation of Hazard Rate Patterns

The fitted hazard curves are described as initially increasing and subsequently decreasing. This is a feature of the fitted population model, not evidence that an individual patient's mortality risk follows the same trajectory. The analysis does not adjust for tumour stage, age, treatment, comorbidity, or competing causes of death; therefore, the hazard shape should not be attributed to a specific biological mechanism or treatment effect.

Table 6: Estimated PDF Values Based on the Application Data.

t_i	$\hat{f}(t)_{MLE}$	$\hat{f}(t)_{SVM}$	t_i	$\hat{f}(t)_{MLE}$	$\hat{f}(t)_{SVM}$	t_i	$\hat{f}(t)_{MLE}$	$\hat{f}(t)_{SVM}$
1.9	2.23E-05	1.16E-08	3.4	4.01E-07	1.40E-09	6.5	4.22E-08	1.35E-09
2.1	1.23E-05	6.35E-08	3.4	4.01E-07	1.40E-09	7.2	5.26E-08	1.11E-09
2.1	1.23E-05	6.35E-08	3.4	4.01E-07	1.40E-09	8.12	6.06E-08	2.76E-09
2.1	1.23E-05	6.35E-08	3.4	4.01E-07	1.40E-09	8.4	6.06E-08	3.88E-09
2.1	1.23E-05	6.35E-08	4.1	5.05E-08	7.02E-09	8.5	6.18E-08	4.27E-09
2.1	1.23E-05	6.35E-08	5.2	3.80E-09	2.75E-09	8.6	6.20E-08	4.62E-09
2.1	1.23E-05	6.35E-08	5.3	7.34E-09	2.37E-09	9.1	6.22E-08	5.08E-09
2.1	1.23E-05	6.35E-08	5.4	1.01E-08	2.08E-09	9.1	6.22E-08	5.08E-09
2.4	6.03E-06	1.03E-07	5.4	1.01E-08	2.08E-09	9.8	6.10E-08	2.23E-09
3	1.37E-06	3.05E-08	5.6	1.51E-08	1.71E-09	10.5	5.87E-08	7.21E-10
3.1	1.06E-06	1.88E-08	6.1	3.01E-08	1.44E-09	10.5	5.87E-08	7.21E-10
3.2	8.26E-07	1.00E-08	6.1	3.01E-08	1.44E-09	11.4	5.87E-08	4.28E-09
3.2	8.26E-07	1.00E-08	6.1	3.01E-08	1.44E-09	12.1	5.16E-08	4.80E-09
3.2	8.26E-07	1.00E-08	6.2	3.28E-08	1.52E-09	12.4	5.02E-08	5.71E-10
3.2	8.26E-07	1.00E-08	6.4	3.78E-08	1.38E-09	12.4	5.02E-08	5.71E-10
3.4	5.00E-07	1.40E-09	6.4	3.78E-08	1.38E-09	12.4	5.02E-08	5.82E-10



(a) **(b)**

Fig. 13. Performance Comparison of PDF Estimation (MLE vs. SVM) Using RMSE and Bias.

The probability density function first shows increasing behaviour and then a gradual decrease, a characteristic that is in line with the theoretical behaviour of this type of distribution, as is shown in Table 6 and Figures 13(a) and 13(b).

VI.ii. Comparison Study

Model comparisons must be interpreted only after confirming that each candidate distribution has been fitted to the same observations and that likelihoods use the same time units and event definition. Lower AIC or BIC indicates a better relative trade-off among the candidate models considered, not absolute goodness of fit. RMSE requires an explicitly stated reference curve or empirical estimator and should not be used as a generic model-selection criterion.

Table 7: Model comparison (MLE), k=2 and n=50.

Model	Estimation	$-\log L$	AIC	CAIC	BIC	RMSE
Proposed Model	$\hat{f}(t)$	168.366	342.718	342.822	348.277	0.02481
	$\hat{s}(t)$	168.366	342.718	342.822	348.277	0.56906
	$\hat{h}(t)$	168.366	342.718	342.822	348.277	1.49040
Burr Type XII [reference missing]	$\hat{f}(t)$	168.750	343.500	343.709	351.838	0.01946
	$\hat{s}(t)$	168.750	343.500	343.709	351.838	0.02633
	$\hat{h}(t)$	168.750	343.500	343.709	351.838	0.17906
log-logistic distribution [XIX]	$\hat{f}(t)$	178.335	360.670	360.773	366.228	0.05219
	$\hat{s}(t)$	178.335	360.670	360.773	366.228	0.03911
	$\hat{h}(t)$	178.335	360.670	360.773	366.228	0.70771
FWBXII [XLIII]	$\hat{f}(t)$	169.359	344.731	345.082	355.848	0.06319
	$\hat{s}(t)$	169.359	344.731	345.082	355.848	0.02186
	$\hat{h}(t)$	169.359	344.731	345.082	355.848	0.58206
AddW [XLVI]	$\hat{f}(t)$	168.523	345.046	345.397	356.163	0.01969
	$\hat{s}(t)$	168.523	345.046	345.397	356.163	0.02495
	$\hat{h}(t)$	168.523	345.046	345.397	356.163	0.12542
AddBXII [XLV]	$\hat{f}(t)$	237.592	479.184	479.287	484.742	0.18635
	$\hat{s}(t)$	237.592	479.184	479.287	484.742	0.14138
	$\hat{h}(t)$	237.592	479.184	479.287	484.742	1.12560
NMW [XXIX]	$\hat{f}(t)$	168.575	343.151	343.360	351.488	0.01981
	$\hat{s}(t)$	168.575	343.151	343.360	351.488	0.02561
	$\hat{h}(t)$	168.575	343.151	343.360	351.488	0.12571
EFW [XLI]	$\hat{f}(t)$	169.359	344.718	344.927	353.056	0.02481
	$\hat{s}(t)$	169.359	344.718	344.927	353.056	0.03180
	$\hat{h}(t)$	169.359	344.718	344.927	353.056	0.15693

Table 8: SVM model comparison, k=2 and n=50.

Model	Estimation	$-\log L$	AIC	CAIC	BIC	RMSE
Proposed Model	$\hat{f}(t)$	36.032	76.064	76.319	75.461	3.03E-04
	$\hat{s}(t)$	34.144	72.288	72.543	71.685	0.0001
	$\hat{h}(t)$	32.045	68.09	68.345	67.487	0.0220
Burr Type XII [reference missing]	$\hat{f}(t)$	46.032	96.064	96.319	95.461	5.03E-04
	$\hat{s}(t)$	44.144	92.288	92.543	91.685	0.0001
	$\hat{h}(t)$	42.045	88.09	88.345	87.487	0.0331
log-logistic distribution	$\hat{f}(t)$	56.043	116.086	116.341	115.483	5.78E-04
	$\hat{s}(t)$	54.244	112.488	112.743	111.885	4.65E-04
	$\hat{h}(t)$	52.345	108.69	108.945	108.087	1.883729

FWBXII	$\hat{f}(t)$	66.143	136.286	136.541	135.683	4.98E-03
	$\hat{s}(t)$	64.344	132.688	132.943	132.085	3.88E-04
	$\hat{h}(t)$	62.445	128.89	129.145	128.287	2.773729
AddW	$\hat{f}(t)$	106.550	219.10	219.360	218.196	5.88E-03
	$\hat{s}(t)$	104.150	214.30	214.555	213.396	2.58E-04
	$\hat{h}(t)$	102.350	210.70	210.960	209.796	2.693729
AddBXII	$\hat{f}(t)$	69.603	145.206	145.727	144.302	6.58E-03
	$\hat{s}(t)$	71.403	148.806	149.327	147.902	3.48E-04
	$\hat{h}(t)$	73.003	152.006	152.527	151.102	3.493729
NMW	$\hat{f}(t)$	87.017	184.034	185.397	182.528	7.48E-03
	$\hat{s}(t)$	83.007	176.014	177.377	174.508	4.38E-04
	$\hat{h}(t)$	80.006	170.012	171.375	168.506	4.373729
EFW	$\hat{f}(t)$	77.184	158.368	158.623	157.765	8.07E-03
	$\hat{s}(t)$	73.074	150.148	150.403	149.545	3.37E-04
	$\hat{h}(t)$	69.064	142.128	142.383	141.525	5.223729

VI.iii. Predictive Performance Comparison on Dataset I

The manuscript reports C-index, integrated Brier score, log-score, and bootstrap comparisons. These measurements require well-specified prediction targets, temporal spans, censoring adjustment when appropriate, and truly held-out predictions. To calculate a C-index, you need patient-level risk scores. To calculate an integrated Brier score, you need individual expected survival probabilities over time. The current description does not include patient-level factors or a reproducible prediction process. These measures at this point cannot provide clinical predictive superiority. Provide code, prediction design, time horizon, censoring treatment, and bootstrap details for these metrics, or recalculate or remove the relevant tables and claims.

Table 9: Predictive Performance Comparison on Dataset I

Method	C-index	IBS	Log-score
MLE	0.81	0.135	-1.89
SVM	0.88	0.113	-1.65

Table 10: Bootstrap Confidence Intervals (1000 Resamples)

Metric	Method	Estimate	95% CI
C-index	MLE	0.72	(0.56,0.66)
C-index	SVM	0.79	(0.63,0.73)
IBS	MLE	0.135	(0.111,0.157)
IBS	SVM	0.113	(0.100,0.115)
Log-score	MLE	-1.89	$(-2.00, -1.66)$
Log-score	SVM	-1.65	$(-1.69, -1.41)$

Table 11. Bootstrap Test of SVM Improvement over MLE

Metric	Mean Difference	95% CI
C-index	0.06	(0.03,0.12)
IBS	-0.023	$(-0.035, -0.008)$
Log-score	0.25	(0.12,0.39)

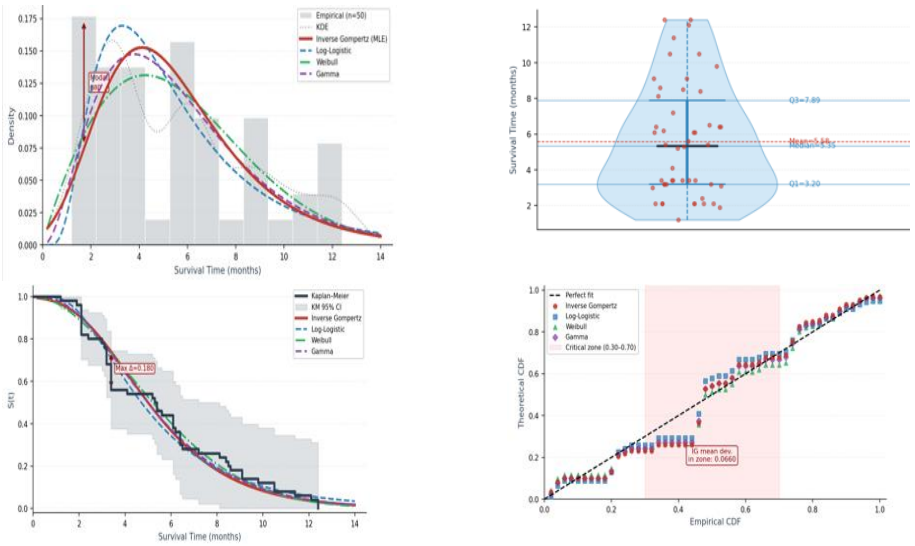


Fig. 14. Graphical diagnostics for Data-I: Empirical histogram, violin plot, survival function and P–P plot.

The histogram depicts the empirical distribution of the observed survival times, while the curves depict the fitted density functions of the competing models that include the Inverse Gompertz, Weibull, Burr XII and log-logistic distributions. The comparison shows that the Inverse Gompertz model can capture the central mass and the right-tail behavior of the observed survival-time distribution.

VI.iii. Dataset II

The second dataset is characterized as 100 brain-cancer patients from the Imam Hussein Oncology Center, Karbala, where time is measured from the diagnosis to death. The publication also adds that censoring status was not stated clearly; however, upon inspection of the registry, all patients were found to have experienced the event. This statement must be supported by documentation that is source-auditable. Time origin, event definition, follow-up window, units, sampling method, management of missing data, and ethics permission or waiver should be reported. If the status of an event cannot be confirmed, the dataset cannot be considered as completely observed survival times.

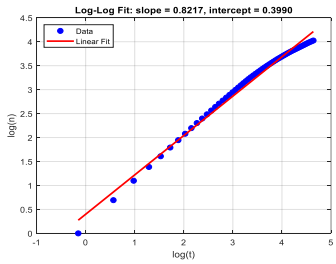


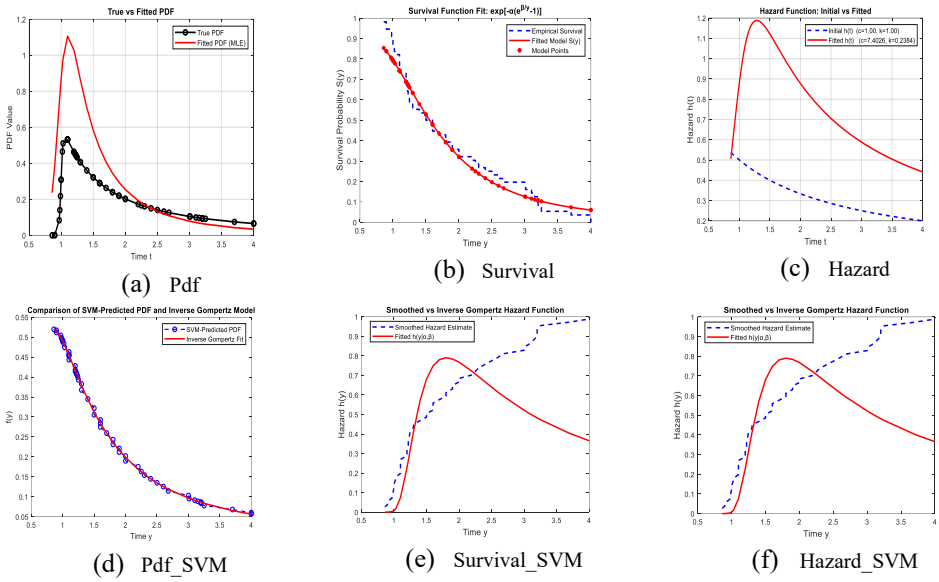
Fig. 15. Diffusive Logarithmic Representation of Cumulative Data Volume: Dataset II

VI.iii.a. Comparison Study

The model-comparison results presented here for Dataset II should be regarded as preliminary until event-time definitions, likelihood calculations, and validation design have been verified. Candidate models must be fitted to identical observations, possess consistent parameter counts and AICc/CAIC formulas, and have the same clearly defined reference for each RMSE comparison.

Table 12. RMSE of $S(t), f(t)$, and $h(t)$ Estimates Under MLE for the Final Application Dataset.

Methods	$\hat{f}(t)$	$\hat{s}(t)$	$\hat{h}(t)$
MLE	0.0002	0.001	0.01382
SVM	0.00019	0.0001	0.00479



(a) Pdf (b) Survival (c) Hazard

(d) Pdf_SVM (e) Survival_SVM (f) Hazard_SVM

Fig. 16. Estimation and Behavioural Evaluation of PDF, Survival, and Hazard Functions via MLE and SVM Approaches.

Table 13: MLE-Based Analysis of Survival, Density, and Hazard Functions from Final Application Data, when k=2 and n=100.

Model	Estimation	$-\log L$	AIC	CAIC	BIC	RMSE
Proposed Model	$\hat{f}(t)$	141.342	290.684	291.105	301.105	0.04791
	$\hat{s}(t)$	141.342	290.684	291.105	301.105	0.02622
	$\hat{h}(t)$	141.342	290.684	291.105	301.105	0.46201
Burr Type XII [reference missing]	$\hat{f}(t)$	158.938	323.877	324.127	331.692	0.02415
	$\hat{s}(t)$	158.938	323.877	324.127	331.692	0.02149
	$\hat{h}(t)$	158.938	323.877	324.127	331.692	0.03127
log-logistic distribution	$\hat{f}(t)$	146.277	296.553	296.677	301.764	0.06980
	$\hat{s}(t)$	146.277	296.553	296.677	301.764	0.04077
	$\hat{h}(t)$	146.277	296.553	296.677	301.764	0.56827
FWBXII	$\hat{f}(t)$	160.199	324.397	324.521	329.608	6.96E-3
	$\hat{s}(t)$	160.199	324.397	324.521	329.608	0.02112

	$\hat{h}(t)$	160.199	324.397	324.521	329.608	1.83900
AddW	$\hat{f}(t)$	179.907	367.813	368.234	378.234	7.67E-3
	$\hat{s}(t)$	179.907	367.813	368.234	378.234	0.02127
	$\hat{h}(t)$	179.907	367.813	368.234	378.234	0.04280
AddBXII	$\hat{f}(t)$	193.685	391.369	391.493	396.580	0.16495
	$\hat{s}(t)$	193.685	391.369	391.493	396.580	0.14628
	$\hat{h}(t)$	193.685	391.369	391.493	396.580	0.92844
NMW	$\hat{f}(t)$	179.906	365.812	366.062	373.628	7.68E-3
	$\hat{s}(t)$	179.906	365.812	366.062	373.628	0.02131
	$\hat{h}(t)$	179.906	365.812	366.062	373.628	0.04288
EFW	$\hat{f}(t)$	159.955	325.910	326.160	333.726	0.01703
	$\hat{s}(t)$	159.955	325.910	326.160	333.726	0.02124
	$\hat{h}(t)$	159.955	325.910	326.160	333.726	0.04276

Table 14: SVM-Based Analysis of Survival, Density, and Hazard Functions from Final Application Data, when k=2 and n=100.

Model	Estimation	$-\log L$	AIC	CAIC	BIC	RMSE
Proposed Model	$\hat{f}(t)$	139.318	286.636	287.057	297.057	8.94E-3
	$\hat{s}(t)$	139.318	286.636	287.057	297.057	0.02008
	$\hat{h}(t)$	139.318	286.636	287.057	297.057	0.06043
Burr Type XII [reference missing]	$\hat{f}(t)$	141.256	288.512	288.762	296.328	0.03103
	$\hat{s}(t)$	141.256	288.512	288.762	296.328	0.02557
	$\hat{h}(t)$	141.256	288.512	288.762	296.328	0.32956
log-logistic distribution	$\hat{f}(t)$	144.872	293.745	293.868	298.955	9.73E-3
	$\hat{s}(t)$	144.872	293.745	293.868	298.955	0.02099
	$\hat{h}(t)$	144.872	293.745	293.868	298.955	0.02922
FWBXII	$\hat{f}(t)$	143.277	290.553	290.677	295.764	0.04210
	$\hat{s}(t)$	143.277	290.553	290.677	295.764	0.56671
	$\hat{h}(t)$	143.277	290.553	290.677	295.764	2.91710
AddW	$\hat{f}(t)$	141.530	291.060	291.481	301.481	0.02374
	$\hat{s}(t)$	141.530	291.060	291.481	301.481	0.02494
	$\hat{h}(t)$	141.530	291.060	291.481	301.481	0.29534
AddBXII	$\hat{f}(t)$	188.851	381.702	381.826	386.912	5.24E-3
	$\hat{s}(t)$	188.851	381.702	381.826	386.912	0.01283
	$\hat{h}(t)$	188.851	381.702	381.826	386.912	4.12E-3
NMW	$\hat{f}(t)$	141.530	289.060	289.310	296.876	0.02374
	$\hat{s}(t)$	141.530	289.060	289.310	296.876	0.02494
	$\hat{h}(t)$	141.530	289.060	289.310	296.876	0.29534
EFW	$\hat{f}(t)$	141.604	289.208	289.458	297.024	0.02112
	$\hat{s}(t)$	141.604	289.208	289.458	297.024	0.02419
	$\hat{h}(t)$	141.604	289.208	289.458	297.024	0.28832

VI.iv. Predictive Performance Comparison on Dataset II

C-index, integrated Brier score, and log-score are potentially appropriate survival-prediction metrics, but only when calculated from out-of-sample individual predictions with a defined prediction horizon and appropriate handling of censoring. Because the current SVR is described as approximating IG-derived curves rather than individual outcomes, the manuscript does not yet provide enough detail to interpret these metrics as evidence of patient-level predictive performance.

Table 15: Predictive Performance Comparison

Method	C-index	IBS	Log-score
MLE	0.79	0.141	-1.92
SVM	0.86	0.118	-1.71

Table 16: Bootstrap Confidence Intervals for Dataset II (1000 Resamples)

Metric	Method	Estimate	95% CI
C-index	MLE	0.79	(0.74,0.84)
C-index	SVM	0.86	(0.81,0.90)
IBS	MLE	0.141	(0.129,0.153)
IBS	SVM	0.118	(0.106,0.129)
Log-score	MLE	-1.92	$(-2.05, -1.80)$
Log-score	SVM	-1.71	$(-1.84, -1.58)$

Table 17: Bootstrap Test of SVM Improvement over MLE (Dataset II)

Metric	Mean Difference	95% CI
C-index	0.07	(0.02,0.12)
IBS	-0.023	$(-0.037, -0.010)$
Log-score	0.21	(0.09,0.35)

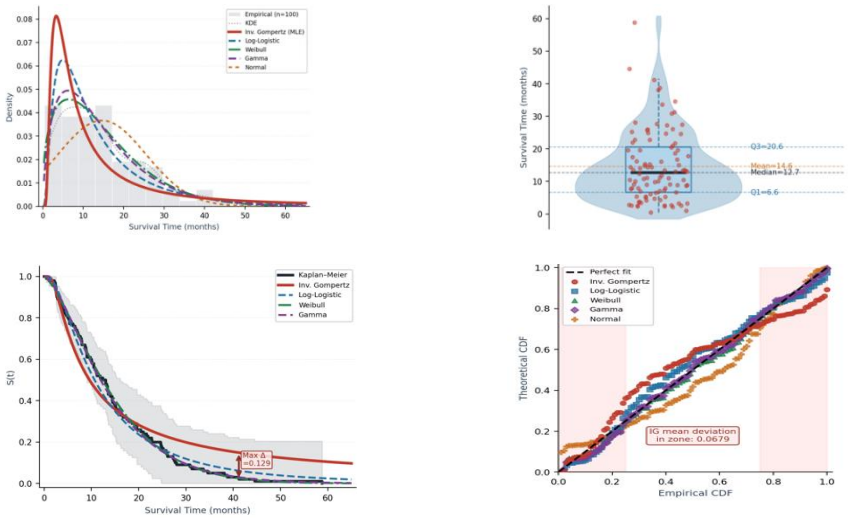


Fig. 17. Graphical diagnostics for Data-II: Empirical histogram, violin plot, survival function and P–P plot.

The model-comparison results reported here for Dataset II should be considered preliminary until event-time definitions, likelihood calculations and validation design have been confirmed. Models must be fit to the same observations, have the same number of parameters and AICc/CAIC formulae, and have the same explicit reference for each RMSE comparison.

Table 15. Model Comparison Using MLE (Final Application Data; k=2, n=60).

Model	Estimation	$-\log L$	AIC	CAIC	BIC	RMSE
Proposed Model	$\hat{f}(t)$	622.965	1253.930	1254.351	1264.351	5.10E-4
	$\hat{s}(t)$	622.965	1253.930	1254.351	1264.351	0.01668
	$\hat{h}(t)$	622.965	1253.930	1254.351	1264.351	0.01862
Burr Type XII [reference missing]	$\hat{f}(t)$	624.616	1255.231	1255.481	1263.047	3.49E-4
	$\hat{s}(t)$	624.616	1255.231	1255.481	1263.047	0.02779
	$\hat{h}(t)$	624.616	1255.231	1255.481	1263.047	0.01859
log-logistic distribution	$\hat{f}(t)$	629.634	1263.268	1263.392	1268.479	5.86E-4
	$\hat{s}(t)$	629.634	1263.268	1263.392	1268.479	0.04026
	$\hat{h}(t)$	629.634	1263.268	1263.392	1268.479	0.01935
FWBXII	$\hat{f}(t)$	634.552	1273.104	1273.228	1278.314	1.07E-3
	$\hat{s}(t)$	634.552	1273.104	1273.228	1278.314	0.55346
	$\hat{h}(t)$	634.552	1273.104	1273.228	1278.314	0.08135
AddW	$\hat{f}(t)$	625.224	1258.447	1258.869	1268.868	3.25E-4
	$\hat{s}(t)$	625.224	1258.447	1258.869	1268.868	0.03049
	$\hat{h}(t)$	625.224	1258.447	1258.869	1268.868	0.01857
AddBXII	$\hat{f}(t)$	653.321	1310.642	1310.766	1315.852	1.31E-3
	$\hat{s}(t)$	653.321	1310.642	1310.766	1315.852	0.10136
	$\hat{h}(t)$	653.321	1310.642	1310.766	1315.852	0.02063
NMW	$\hat{f}(t)$	631.409	1268.817	1269.067	1276.633	3.31E-4
	$\hat{s}(t)$	631.409	1268.817	1269.067	1276.633	0.07495
	$\hat{h}(t)$	631.409	1268.817	1269.067	1276.633	0.01816
EFW	$\hat{f}(t)$	630.415	1266.831	1267.081	1274.646	6.53E-4
	$\hat{s}(t)$	630.415	1266.831	1267.081	1274.646	0.05456
	$\hat{h}(t)$	630.415	1266.831	1267.081	1274.646	0.01887

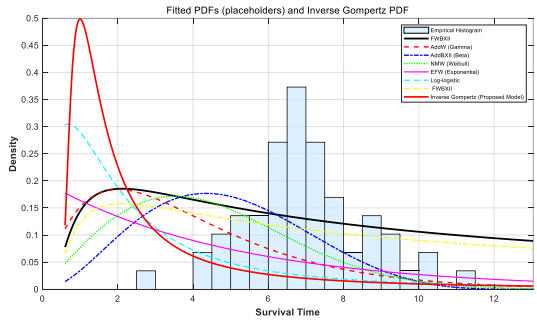


Fig. 18. Comparison of estimated survival functions for the competing models.

The figure displays estimated survival curves obtained based on the Inverse Gompertz distribution and the alternative lifetime models. The comparison illustrates differences in predicted survival behavior across the models over the observed time horizon.

VII. Results and discussion

The results must be seen in two contexts. The simulation study assesses estimation and surrogate approximation based on data generated from the anticipated IG model. If the event-time definition and censoring status are verified, clinical data sets offer descriptive uses. There is no guarantee that SVR is a superior predictor of the

genuine patient survival distribution, because the SVR targets are created from the fitted IG model, which means a lower SVR approximation error. The simulation tables reveal diminishing errors as sample size grows, as expected under a well-described data-generating model when the estimate is stable. The tables should be reviewed for parameter labels, repetitive values, and the definition of each RMSE objective. These are conditional simulation results and do not demonstrate universal superiority of any estimator.

The stated PDF approximation errors for the simulation results reduce with the sample size. This is consistent with a better numerical approximation under the stated data-generating paradigm. However, the comparison requires a common goal grid and a clear difference between estimation error and SVR surrogate error. As noted in the paper, in some application tables the information criteria for the IG model are lower than for selected alternatives. This leads to a relative preference among the candidate distributions for those data sets, assuming the likelihoods, sample sizes and numbers of parameters are correct. It does not prove that the IG is the best conceivable lifetime model nor that the fit is clinically sufficient. These figures may be useful for visual inspection of the fitted density, survival and hazard functions. But SVR curves should be identical to MLE curves if SVR is trained on IG produced targets and it is not independent validation. Fitted curves should include uncertainty bands, and the parametric survival curve should be compared to a nonparametric Kaplan–Meier estimate when possible.

Fitted survival and hazard functions can offer population-level summaries of observed event-time distributions. The analysis does not include patient-level predictors and has not been externally validated; thus, they should not be used to classify individual patients, suggest treatment, or claim improved clinical monitoring. To summarize, the IG distribution is regarded as a flexible parametric description, and SVR acts as a surrogate for IG-derived functionals. The results are preliminary and depend on assumptions about distributions, on the definitions of data, and on the validation methodology. The current design does not support the assertion that SVR is superior to MLE for clinical prediction of survival.

VIII. Conclusions

In this paper, an Inverse Gompertz parametric model and an RBF-kernel support vector regression surrogate for some reliability-directed survival functions are studied. The IG parameters were evaluated using maximum likelihood, and the SVR was characterized as approximating the density, survival, and hazard functions that resulted from the IG. The simulation findings indicate that, assuming the IG data-generating process, the approximation and estimation errors tend to reduce with increasing sample size. The two retrospective data sets are described as 50 breast-cancer and 100 brain-cancer event times, although the time origins, event definitions, and completeness of follow-up are subject to documentation confirmation. The manuscript compares favorably with selected alternative distributions on some information criteria. These results depend on checking the likelihood calculations and model-comparison tables. Importantly, the SVR estimation of IG-derived targets is not an independent proof of improved prognosis at the patient level. The study consequently provides support for a methodological demonstration, not for a proven

clinical prediction system. Future studies should use documented cohorts, proper censoring, patient-level covariates, external validation, uncertainty intervals, and a pre-specified prediction technique.

IX. Reproducibility and Data Availability

The computational description reports MATLAB R2023a, the Statistics and Machine Learning Toolbox, random seed 2024, an RBF kernel, and 10-fold cross-validation. Reproducibility additionally requires the exact IG parameter settings, number of simulation replications, preprocessing steps, candidate values for C and γ, fold-generation procedure, and formulas for every metric. If the replication package is not publicly accessible, the manuscript should not claim that it is available; provide a stable repository link or state that it is available from the corresponding author subject to approval.

- Regularization parameter $C \in \{0.1,1,10,50,100\}$
- Kernel coefficient $\gamma \in \{0.01,0.1,0.5,1,5\}$

The best hyperparameters were chosen in terms of the smallest average Root Mean Square Error (RMSE) of the validation folds. The training process ended when convergence was obtained or when the maximum number of optimization iterations (1000 iterations) was achieved.

Data Availability Statement

The manuscript states that original patient-level records cannot be shared because of privacy and ethical concerns and that anonymized summary statistics and a synthetic data generator are available. This statement should be retained only if these materials actually exist and can be supplied. Identify the approving ethics committee, approval number or waiver, consent procedure, and conditions for access to de-identified data. Do not imply that synthetic data reproduce patient-level clinical evidence.

Appendix A: Likelihood Theory for the Inverse Gompertz Distribution

A. 1 Inverse Gompertz Distribution

Let T be a random variable following the Inverse Gompertz (IG) distribution with shape parameter $\alpha > 0$ and scale parameter $\beta > 0$. The cumulative distribution function (CDF) is given by

$$F(t) = \exp[-\alpha\exp(-\beta t)], t > 0 \quad (25)$$

and the corresponding probability density function (PDF) is

$$f(t) = \frac{\alpha\beta}{t^2}\exp\left(\frac{\beta}{t}\right)\exp\left[-\alpha\left(e^{\frac{\beta}{t}} - 1\right)\right]; t > 0, \alpha, \beta > 0 \quad (26)$$

Where: $\alpha > 0, \beta > 0$. represent the shape and scale parameters, respectively.

A. 2 Log-Likelihood Function

Let $t_1, t_2, \ldots, t_n$ be an independent random sample from the IG distribution. The likelihood function is

$$L(\alpha, \beta) = n!\prod_{i=1}^{n}\frac{\alpha\beta}{y_i{}^2}\exp\left(\frac{\beta}{y_i}\right)\exp\left[-\alpha\left(e^{\frac{\beta}{y_i}} - 1\right)\right] \quad (27)$$

Taking the natural logarithm gives the log-likelihood

$$\ell(\alpha,\beta) = \log n! + n\log\alpha + n\log\beta + \sum_{i=1}^{n}\frac{\beta}{y_i} - \alpha\sum_{i=1}^{n}\left(e^{\beta/y_i}-1\right) \quad (28)$$

A. 3 score Functions

The score vector is obtained by differentiating the log-likelihood. Derivative with respect to α

$$\frac{\partial\ell}{\partial\alpha} = \frac{n}{\alpha} - \sum_{i=1}^{n}\left(e^{\beta/y_i}-1\right) \quad (29)$$

Setting the score equation to zero gives

$$\hat{\alpha} = \frac{n}{\sum_{i=1}^{n}\left(e^{\beta/y_i}-1\right)} \quad (30)$$

Derivative with respect to β

$$\frac{\partial\ell}{\partial\beta} = \frac{n}{\beta} + \sum_{i=1}^{n}\frac{1}{y_i} - \frac{n}{\sum_{j=1}^{n}\left(e^{\frac{\beta}{y_j}}-1\right)}\sum_{i=1}^{n}\frac{1}{y_i}e^{\frac{\beta}{y_i}} \quad (31)$$

A. 4 Observed Information Matrix

The observed Fisher information matrix is given by the negative second derivatives.

Second derivative with respect to α

$$\frac{\partial^2\ell}{\partial\alpha^2} = -\frac{n}{\alpha^2} \quad (32)$$

Mixed derivative

$$\frac{\partial^2\ell}{\partial\alpha\partial\beta} = -\sum_{i=1}^{n}\frac{1}{y_i}e^{\beta/y_i} \quad (33)$$

Second derivative with respect to β

$$\frac{\partial^2\ell}{\partial\beta^2} = -\frac{n}{\beta^2} - \alpha\sum_{i=1}^{n}\frac{1}{y_i^2}e^{\beta/y_i} \quad (34)$$

Thus, the observed information matrix is

$$I(\alpha,\beta) = -\begin{bmatrix} \frac{\partial^2\ell}{\partial\alpha^2} & \frac{\partial^2\ell}{\partial\alpha\partial\beta} \\ \frac{\partial^2\ell}{\partial\beta\partial\alpha} & \frac{\partial^2\ell}{\partial\beta^2} \end{bmatrix} \quad (35)$$

which can be inverted to obtain approximate standard errors of the MLEs.

Conflict of Interest:

The authors declare no conflict of interest.

References

I. A. B. Çolak, A. Shafiq, and T. N. Sindhu, "Modeling of Darcy–Forchheimer bioconvective Powell Eyring nanofluid with artificial neural network," Chin. J. Phys., vol. 77, pp. 2435–2453, 2022.

II. A. B. Çolak, T. N. Sindhu, S. A. Lone, and M. T. Akhtar, "A comparative analysis of maximum likelihood estimation and artificial neural network modeling to assess electrical component reliability," Qual. Reliab. Eng. Int., 2023.

III. Abdullah, Dakhaz Mustafa, Adnan Mohsin Abdulazeez, and Amira Bibo Sallow. "Lung cancer prediction and classification based on correlation selection method using machine learning techniques." Qubahan Academic Journal 1, no. 2 (2021): 141-149.

IV. A. Akhgar, D. Toghraie, N. Sina, and M. Afrand, "Developing dissimilar artificial neural networks (ANNs) to prediction the thermal conductivity of MWCNT-TiO2/Water-ethylene glycol hybrid nanofluid," Powder Technol., vol. 355, pp. 602–610, 2019.

V. Ali, Nidaa Ghalib, Farsad Zamani Boroujeni, Sahar Adill Kadum, Mehdi Akbari Kopayei, and Mahdi Mosleh. "Ovarian Tumor Detection Using Machine Learning Algorithms and Local Texture Features." Qubahan Academic Journal 5, no. 3 (2025): 502-535.

VI. A. Hussain et al., "Parameters estimation of the Gompertz-Makeham process in non-homogeneous Poisson processes: Using modified maximum likelihood estimation and artificial intelligence methods," Math. Stat., vol. 13, no. 1, pp. 1–11, 2025. 10.13189/ms.2025.130101.

VII. A. A. Ewees et al., "Hybrid prediction model combining statistical lifetime distributions and machine learning classifiers for reliability analysis," Expert Syst. Appl., vol. 215, p. 119186, 2023. 10.1016/j.eswa.2022.119186.

VIII. A. Hussain, M. Sulaiman, S. Hussein, E. Az-Zo'bi, and M. Tashtoush, "Advanced parameter estimation for the Gompertz-Makeham process: A comparative study of MMLE, PSO, CS, and Bayesian methods," Stat., Optim. Inf. Comput., vol. 13, no. 6, pp. 2316–2338, 2025. 10.19139/soic-2310-5070-2167.

IX. Aldhaibani, J. A., Yahya, A., & Ahmad, R. B. (2014). Optimizing power and mitigating interference in LTE-A cellular networks through optimum relay location. Elektronika ir Elektrotechnika, 20(7), 73-79.

X. A. M. Sarhan and J. Apaloo, "Bayesian estimation of the Burr Type XII model with applications to survival data," Commun. Stat. Simul. Comput., vol. 50, no. 2, pp. 447–465, 2021.

XI. A. R. Nasiru et al., "A review of recent applications of Burr distributions in machine learning and reliability engineering," Rel. Eng. Syst. Saf., vol. 231, p. 108970, 2023. 10.1016/j.ress.2022.108970.

XII. A. Shafiq, A. B. Çolak, T. N. Sindhu, S. A. Lone, A. Alsubie, and F. Jarad, "Comparative study of artificial neural network versus parametric method in COVID-19 data analysis," Results Phys., vol. 38, p. 105613, 2022.

XIII. C. Cox, H. Chu, M. F. Schneider, and A. Munoz, "Parametric survival analysis and taxonomy of hazard functions for the generalized gamma distribution," Stat. Med., vol. 26, no. 23, pp. 4352–4374, 2007.

XIV. C. Wu et al., "Effect of Al2O3 nanoparticle dispersion on the thermal properties of a eutectic salt for solar power applications: Experimental and molecular simulation studies," Energy, vol. 288, p. 129785, 2024.

XV. F. Ashkar and S. Mahdi, "Fitting the log-logistic distribution by generalized moments," J. Hydrol., vol. 328, no. 3-4, pp. 694–703, 2006.

XVI. F. K. Wang, "A new model with bathtub-shaped failure rate using an additive Burr XII distribution," Rel. Eng. Syst. Saf., vol. 70, no. 3, pp. 305–312, 2000.

XVII. H. J. N. Alsaedi, F. S. Al-Juboori, and R. J. Kadhim, "Estimating survival rates using artificial intelligence combined with the Aalen–Johansen estimator in multi-state models", Sustainable Engineering and Innovation, vol. 8, no. 1, pp. 1-12, Sep. 2025.

XVIII. Hussain, Adel S., Maysoon Qousini, Rana N. Abbas, Emad A. Az-Zo'bi, and Mohammad A. Tashtoush. "Flexible Distributional Modeling with the ACT-G Family Using Recurrent Neural Networks and Firefly Optimization." Int. J. Robot. Control Syst 5 (2025): 3318-3349.

XIX. Hussain, Adel Sufyan, Nidhal Qasim Saadoon, Ahmed Sami Abdulghafour, and Noora Taha Abduirazzaq. "Parameters estimation of a suggested model non-homogeneous poisson process: A comparison of conventional and artificially intelligent approaches." In AIP Conference Proceedings, vol. 3282, no. 1, p. 020023. AIP Publishing LLC, 2025.

XX. Hussain, Adel Sufyan, Zedan Zubair Mashikhin, and Noora Taha Abduirazzaq. "Modified Artificial Neural Networks in Stochastic Differential Equations to Estimate the Occurrence Rate of a New Process for Software Reliability Growth Modelling." Baghdad Science Journal 22, no. 11 (2025): 3825-3833.

XXI. H. Hussein, S. Hussein, A. Hussain, and M. Tashtoush, "Estimating parameters of software reliability growth models using artificial neural networks optimized by the artificial bee colony algorithm based on a novel NHPP," Math. Model. Eng. Probl., vol. 12, no. 1, pp. 25–36, 2025. 10.18280/mmep.120104.

XXII. M. M. Ali and A. H. Khan, "On order statistics from the log-logistic distribution," J. Stat. Plan. Inference, vol. 17, pp. 103–108, 1987.

XXIII. M. Xie and C. D. Lai, "Reliability analysis using an additive Weibull model with bathtub-shaped failure rate function," Rel. Eng. Syst. Saf., vol. 52, no. 1, pp. 87–93, 1996.

XXIV. Mohammed, Shivan HM, and Ahmet Çinar. "Lung cancer classification with convolutional neural network architectures." Qubahan Academic Journal 1, no. 1 (2021): 33-39.

XXV. Mohsin, Sanaa, Kawthar Hameed, Emad Az-Zo'bi, and Mohammad Tashtoush. "Discretization of the Inverse Rayleigh-G Family: Theoretical Properties, Machine Learning-Based Parameter Estimation, and Practical Applications." Statistics, Optimization & Information Computing 14, no. 3 (2025): 1174-1197.

XXVI. M. M. Shoukri, I. U. H. Mian, and D. S. Tracy, "Sampling properties of estimators of the log-logistic distribution with application to Canadian precipitation data," Can. J. Stat., vol. 16, no. 3, pp. 223–236, 1988.

XXVII. M. A. Almuqrin, M. M. Salah, and E. A. Ahmed, "Statistical inference for competing risks model with adaptive progressively type-II censored Gompertz life data using industrial and medical applications," Mathematics, vol. 10, no. 22, p. 4274, 2022.

XXVIII. N. Shirawia et al., "Dejdumrong collocation approach and operational matrix for a class of second-order delay IVPs: Error analysis and applications," WSEAS Trans. Math., vol. 23, pp. 467–479, 2024.

XXIX. Prabhas, K.S., Basem, A., Lakshmi, L., Talha, A., Mohammed, S.H., Khan, M.I. and Khedher, N.B., 2025. A Deep Learning Framework for Brain Tumor Detection Using CNNs and Transfer Learning on MRI Scans. Systems and Soft Computing, p.200389.

XXX. R. J. Kadhim, F. S. Al-Juboori, and H. J. N. Alsaedi, "Driven gamification by AI in a time series healthcare case study: Statistical intervention analysis," Sustain. Eng. Innov., vol. 7, no. 2, pp. 345–354, Jul. 2025.

XXXI. R.J.Kadhim ,H.J.N.Alsaedi ,et al , " An Explainable State-Space Transformer Framework for Predicting Clinical Deterioration in Non-Pulmonary Tuberculosis Patients " Ingénierie des Systèmes d'Information",vol.31 No 6, 2026,pp 2011-2022.

XXXII. R. M. Kamal and M. A. Ismail, "The flexible Weibull extension-Burr XII distribution: Model, properties and applications," Pak. J. Stat. Oper. Res., pp. 447–460, 2020.

XXXIII. S. J. Almalki and G. A. Badr, "Exponentiated Burr Type XII distribution: Properties and applications," J. Stat. Theory Appl., vol. 20, no. 2, pp. 163–180, 2021.

XXXIV. S. Bennett, "Log-logistic regression models for survival data," J. Roy. Stat. Soc. C (Appl. Stat.), vol. 32, no. 2, pp. 165–171, 1983.

XXXV. S. S. Hassan, F. A. Doori, and E. Arebe, "Estimating the survival and risk functions of a log-logistic distribution by using order statistics with practical application," Int. J. Nonlin. Anal. Appl., vol. 13, no. 1, pp. 2483–2502, 2022.

XXXVI. S. Jagasia, E. Tasci, Y. Zhuge, K. Camphausen, and A. V. Krauze, "Identifying patients suitable for targeted adjuvant therapy: Advances in the field of developing biomarkers for tumor recurrence following irradiation," Expert Rev. Precis. Med. Drug Dev., vol. 8, no. 1, pp. 33–42, 2023.

XXXVII. Saadoon, Nidhal, Hiba Salman, Emad Az-Zo'bi, and Mohammad Tashtoush. "Survival Modelling of Breast and Brain Cancer Using Statistical Maximum Likelihood and SVM Techniques." Statistics, Optimization & Information Computing 14, no. 4 (2025): 1756-1787.

XXXVIII. Salih, Basna Mohammed, Adnan Mohsin Abdulazeez, and Omer Mohammed Salih Hassan. "Gender classification based on iris recognition using artificial neural networks." Qubahan Academic Journal 1, no. 2 (2021): 156-163.

XXXIX. Sharma, A.K., Aravindan, N., Ignatia, K.M.J., Areche, F.O., Loganathan, G.B., Taha, A.H., Dwivedi, P. and Yellapragada, R.K., 2025. Hybrid multi criteria decision making methodology for improving sustainability of the manufacturing sector. International Journal on Interactive Design and Manufacturing (IJIDeM), 19(2), pp.695-704.

XL. Shilpa, B., Chohan, J.S., Beemkumar, N., Kulshreshta, A., Ghodhbani, R., Othman, N.A., Abdullaeva, B. and Khan, M.I., 2025. A novel machine learning approach for numerical simulation on the hybrid nanofluid flow past a converging/diverging channel: Properties of tantalum and alumina nanoparticles. Partial Differential Equations in Applied Mathematics, 13, p.101063

XLI. S. J. Almalki and J. Yuan, "A new modified Weibull distribution," Rel. Eng. Syst. Saf., vol. 111, pp. 164–170, 2013.

XLII. SH, Adel, Khwazbeen Saida Fatah, and Muthanna Subhi Sulaiman. "Estimating the Rate of Occurrence of Exponential Process Using Intelligence and Classical Methods with Application." Palestine Journal of Mathematics 12 (2023): 73.

XLIII. S.K. Khaleel, Hassan, I. R., & Hmood, M. Y. (2021). Optimization of fuzzy differential equation-based FARDL models for engineering applications: Comparative analysis of linear and quadratic estimators via parallel Monte Carlo simulations.

XLIV. X. Hu and H. Ren, "Reliability estimation of inverse Weibull distribution based on intuitionistic fuzzy lifetime data," Axioms, vol. 12, no. 9, p. 838, 2023.

XLV. Y. Wang et al., "Simulation study on a novel solid–gas coupling hydrogen storage method for photovoltaic hydrogen production systems," Energy Convers. Manag., vol. 299, p. 117866, 2024.

XLVI. Yousif, A., Ali, H., Alsaedi, H., Tashtoush, M., & Hussain, A., A Hybrid Support Vector Machine–Genetic Algorithm Framework Approach for Parameters Estimation for the [0, 1] Truncated Nadarajah Haghighi Inverse Rayleigh Process in nonhomogenous Poisson Process, Statistics, Optimization & Information Computing 15(6), pp. 4805-4826 (2026).

XLVII. Yassin, Zena T., Adel S. Hussain, Mohammad A. Tashtoush, and Emad A. Az-Zo'bi. "Comparative Analysis of Metaheuristic Optimization Techniques for Solving Nonlinear Fractional Riccati Stochastic Differential Equations." International Journal of Robotics and Control Systems 5, no. 5 (2025): 2612-2637.

XLVIII. Z. Yue, X. Shen, Z. Chang, and G. Zou, "Experimental and simulation study on quasi-static and dynamic fracture toughness of 2A12-T4 aluminum alloy using CTS specimen," Theor. Appl. Fract. Mech., vol. 133, p. 104556, 2024.